A Comparison of Traditional, Step-Path, and Geostatistical Techniques in the Stability Analysis of a Large Open Pit

Mayer J.M.
SRK Consulting (Canada) Inc., Vancouver, BC, Canada, V6E 3X2. Email: jmayer@srk.com

Stead D.
Department of Earth Sciences, Simon Fraser University, Burnaby, BC, Canada, V5A 1S6

ABSTRACT: With the increased drive towards deeper and more complex mine designs, geotechnical engineers are often forced to reconsider traditional deterministic design techniques in favour of probabilistic methods. These alternative techniques allow for the direct quantification of uncertainties within a risk and/or decision analysis framework. However, conventional probabilistic practices typically discretize geological materials into discrete, homogeneous domains, with attributes defined by spatially constant random variables, despite the fact that geological media display inherent heterogeneous spatial characteristics. This research directly simulates this phenomenon using a geostatistical approach, known as sequential Gaussian simulation. The method utilizes the variogram which imposes a degree of controlled spatial heterogeneity on the system. Simulations are constrained using data from the Ok Tedi mine site in Papua New Guinea and designed to randomly vary the geological strength index and uniaxial compressive strength using Monte Carlo techniques. Results suggest that conventional probabilistic techniques have a fundamental limitation compared to geostatistical approaches, as they fail to account for the spatial dependencies inherent to geotechnical datasets. This can result in erroneous model predictions, which are overly conservative when compared to the geostatistical results.

KEYWORDS: rock mass; large open pits; reliability based design; geostatistics; heterogeneity; probabilistic methods

CITATION: Mayer, J.M., and D. Stead. 2017. A comparison of traditional, step-path, and geostatistical techniques in the stability analysis of a large open pit. Rock Mechanics and Rock Engineering. 50:927-949.

This is the author's version of the original manuscript.
The final publication is available at Springer via http://dx.doi.org/10.1007/s00603-016-1148-0

1. INTRODUCTION

Geotechnical design projects often suffer from inherent information deficiencies associated with the difficulties and often impractical nature of collecting large datasets (Read 2009, Read and Stacey 2009). This leads to fundamental issues where geotechnical design must be conducted with incomplete knowledge of the true state of the system. Multiple realizations of the subsurface are often possible within the framework of the given state of information. To overcome this deficiency, reliability and/or probability based methods can be used, whereby uncertainty in the capacity and demand is explicitly propagated through design calculations (Harr 1996; Duncan 2000; Wiles 2006; Nadim 2007). Conventional practice dictates the geological medium should be subdivided into a series of geotechnical units whose properties are defined by spatially constant random variables (Read and Stacey 2009). However, an underlying uncertainty is introduced into the design process as the scale of data collection and analysis often differ resulting in data aggregation issues (Gehlke and Biehl 1934; Yule and Kendall 1950; Clark and Avery 1976; Haining 2003). These issues are exacerbated by the application of classical statistical methods and the false assumption of data independence, despite the inherent spatial variability within natural geological systems (Journel and Huijbregts 1978; Isaaks and Srivastava 1989; Deutsch 2002). Such oversimplification of the spatial heterogeneity favors conservative design practices, with an over-estimation of the probability of failure (Griffiths and Fenton 2000; Hicks and Samy 2002). The result is the inability to reproduce realistic failure paths, as the lack of heterogeneity prevents the development of step-path failures through the weakest areas of the rock mass (Jefferies et al. 2008; Lorig 2009).

Techniques have been proposed to incorporate spatial heterogeneity including explicit modelling within geomechanical simulations (Baczynski 1980; Pascoe et al. 1998; Jefferies et al. 2008; Srivastava 2012), and the use of critical path algorithms for statistical upscaling of attribute distributions (Glynn et al. 1978; Glynn 1979; O'Reilly 1980; Shair 1981; Einstein et al. 1983; Baczynski 2000; Baczynski 2008). Both methods aim to propagate spatial uncertainties through the geomechanical design calculations using stochastic techniques. However, a fundamental difference exists,

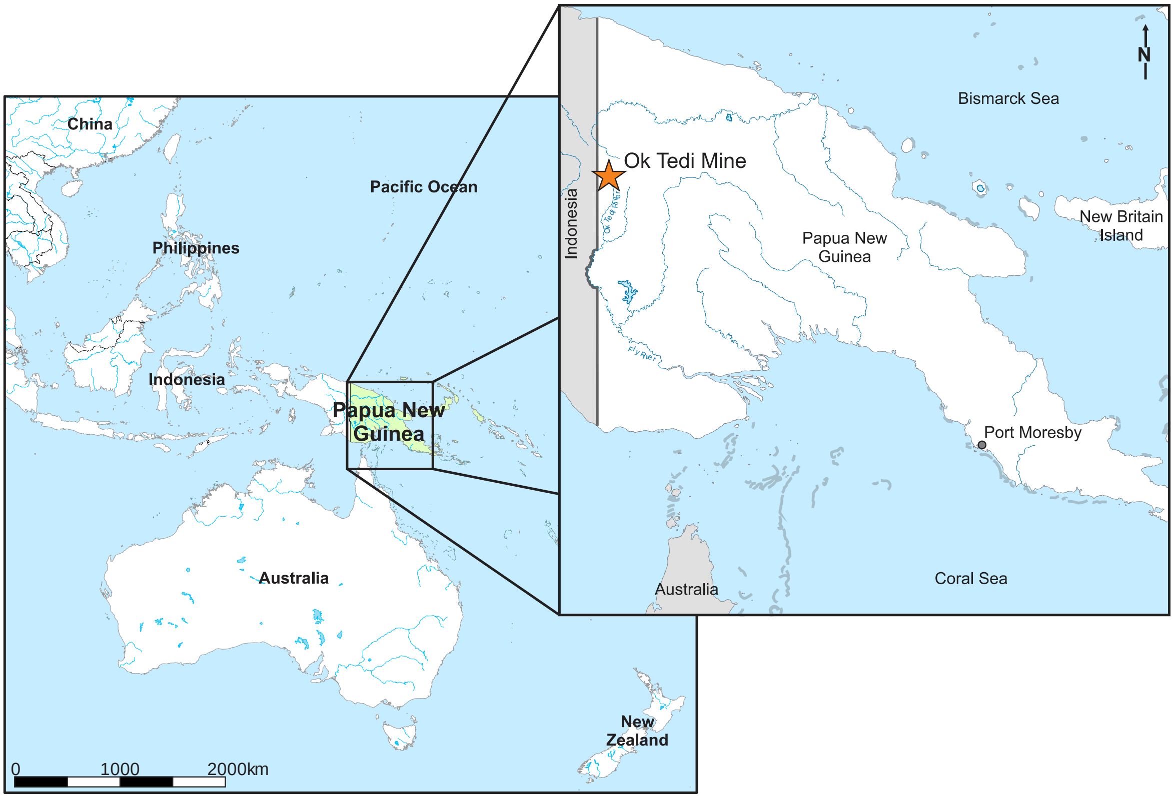

Fig. 1. Location of Ok Tedi Mine in Papua New Guinea.

as the former explicitly models the heterogeneities within the numerical simulations package, while the latter adjusts the attribute statistics prior to their incorporation.

Research attempts to illustrate the limitations of conventional probabilistic design practice and statistical upscaling techniques in the simulation of spatial heterogeneity. A novel approach has been adapted for field of open pit slope design known as sequential Gaussian simulation (SGS), which uses variograms to constrain spatial co-dependencies within the dataset (Journel and Huijbregts 1978; Isaaks and Srivastava 1989; Deutsch 2002; Nowak and Verly 2007). Stochastic techniques are used to construct multiple realizations of the subsurface geological strength index (GSI) and uniaxial compressive strength (UCS) attributes at the Ok Tedi mine site in Papua New Guinea. Such simulations are conducted directly within the geomechanical code, FLAC, which is used to estimate the pit wall stability (Itasca 2011). Results are compared with conventional probabilistic and statistical upscaling techniques to show the limitations of traditional methods.

2. STUDY SITE

The Ok Tedi mine is a copper porphyry deposit which has been in operation since the mid-1980s. The site is located in the remote Western Province of Papua New Guinea, near the border with Indonesia (Bamford 1972; Davies et al. 1978; Figure 1). Situated on top of Mt. Fubilan at an elevation of 1800 m, the site is surrounded by rugged geomorphic features forming a complex irregular topography (Hearn 1995). The mountainous topography coupled with tropical latitude results, by world mining standards, in very adverse climatic conditions, with the mine surrounded by dense tropical rain forest and an annual rainfall of 9 to 11 m (de Bruyn et al. 2011). Active uplift associated with the collision of the Australian and Pacific tectonic plates results in the area experiencing moderate earthquake risks, with events typically ranging between 4 and 6 on the Richter scale (Baczynski et al. 2011).

The current areal extent of the pit is approximately 2000 by 3000 m, with a maximum wall height of 800 m (de Bruyn et al. 2011). A final depth of 900 m is designated for end of life operations; however, a decision is pending to extend this to 1000 m, through a 200 to 300 m pushback of the west wall (de Bruyn et al. 2013). Slope angles average 40° throughout the current pit, with the proposed cut-back designated to 38° to 39°. Conditions of all the pit walls are generally poor due to the high rates of weathering associated with the large amount of rainfall within the area.

The geology of the Ok Tedi mine site is characterised by a repeating succession of sub-horizontal sedimentary facies, which have been locally intruded by two igneous bodies (Figure 2; Figure 3; de Bruyn et al. 2011; Baczynski et al. 2011). Sedimentary facies have been separated into three distinct units, namely: the Ieru Siltstone, Darai Limestone and Pnyang Formation (Hearn 1995). The Ieru Siltstone Formation is characterized by grey, calcareous siltstones, interbedded with minor medium graded sandstones of Cretaceous age. The unit varies in thickness across the site, up to a maximum of 1500 m. The unit is overlain disconformably by a late-Miocene to mid-Eocene, massive, foraminiferal, carbonate-rich packstone, mudstone and wackestone unit, referred to as the Darai Limestone. The limestone varies in thickness from 50 to 800 m across the site, and structurally underlies the mid-Miocene Pnyang Formation. The Pnyang Formation is the youngest of the main sedimentary units found, and is composed of calcareous mudstone and siltstone with minor amounts of limestone.

The boundary between the Ieru Siltstone and Darai Limestone is characterized by a series of low angle thrust faults, referred to as the Taranki, Parrot's Beak and Basal Thrust Zones (Figure 3; Baczynski et al. 2011). The faults are the result of uplift associated with the collision of the Australian and Pacific plates (Fagerlund et al. 2013). The geology is characterized by 20 to 80 m thick zones of highly fractured and altered fault gouge, pyrite, magnetite skarn lenses, brecciated monzodiorite and brecciated siltstone hornfels (de Bruyn et al. 2011). Sedimentary units dip gently towards the southwest, with all three thrust zones exposed in the west wall.

In addition to the three thrust faults, the west wall is cross-cut by two steeply dipping (70º to 80º) sub-vertical faults, referred to as the western (upper) and eastern (lower) Gleeson's faults (de Bruyn et al. 2013; Figure 3). The faults strike approximately parallel to the western pit wall. Displacement along the faults has resulted in the formation of a discrete fracture zone, bound on each side by the respective faults. The rock mass within the zone is highly disturbed and characterized by weak, heavily fractured, brecciated rock, with localized stronger material (Baczynski et al. 2011). The two bounding faults are characterized by highly brecciated, granular and/or highly plastic gouge material. The west wall is also crosscut by several additional, orthogonally oriented, high angle faults, which act as possible release structures for potential slope failures.

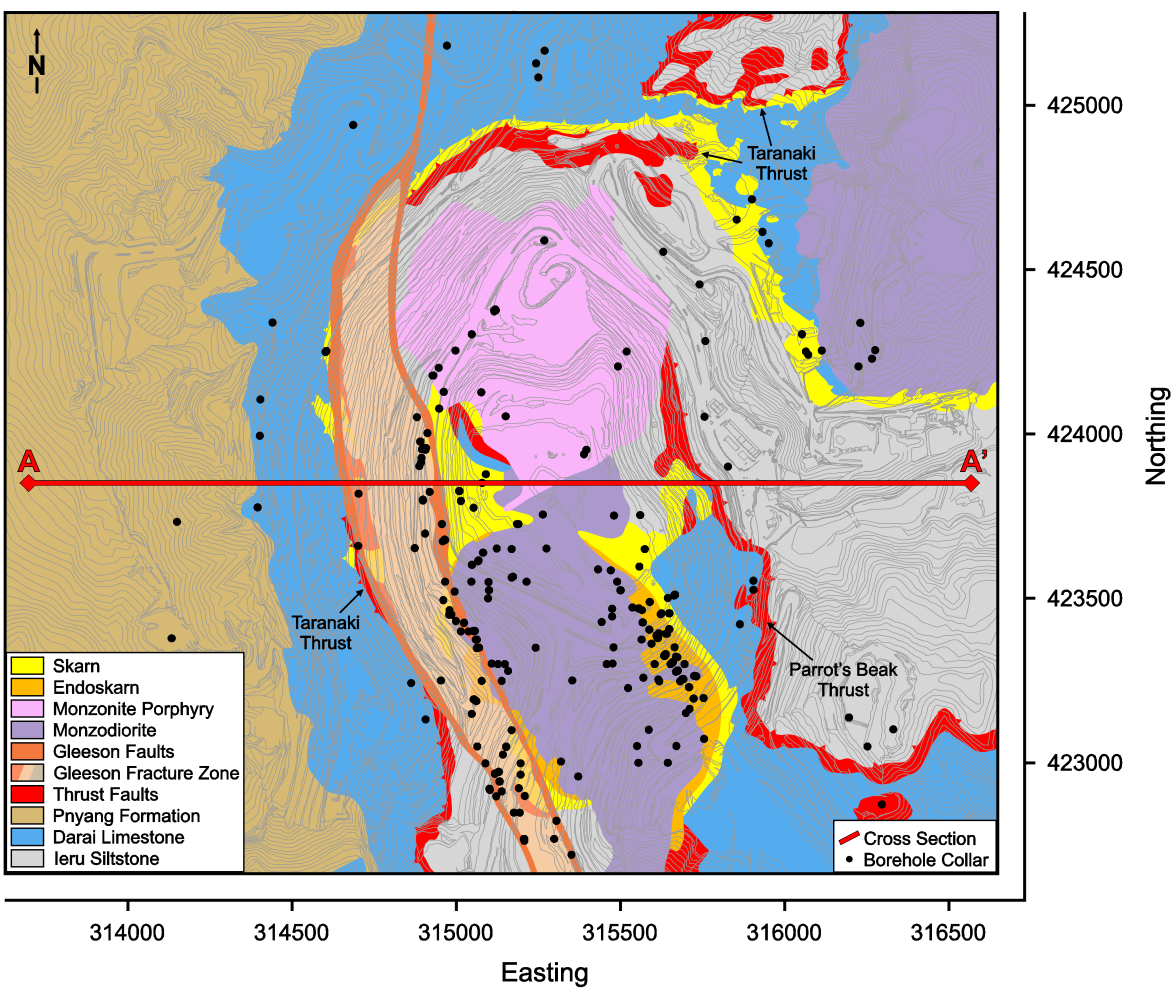

Fig. 2. Plan view of surface geology for the 2011 mining conditions at the Ok Tedi site. The geotechnical borehole collar distribution is found to be skewed towards the centre of the pit, specifically targeting the mineralized skarn bodies.

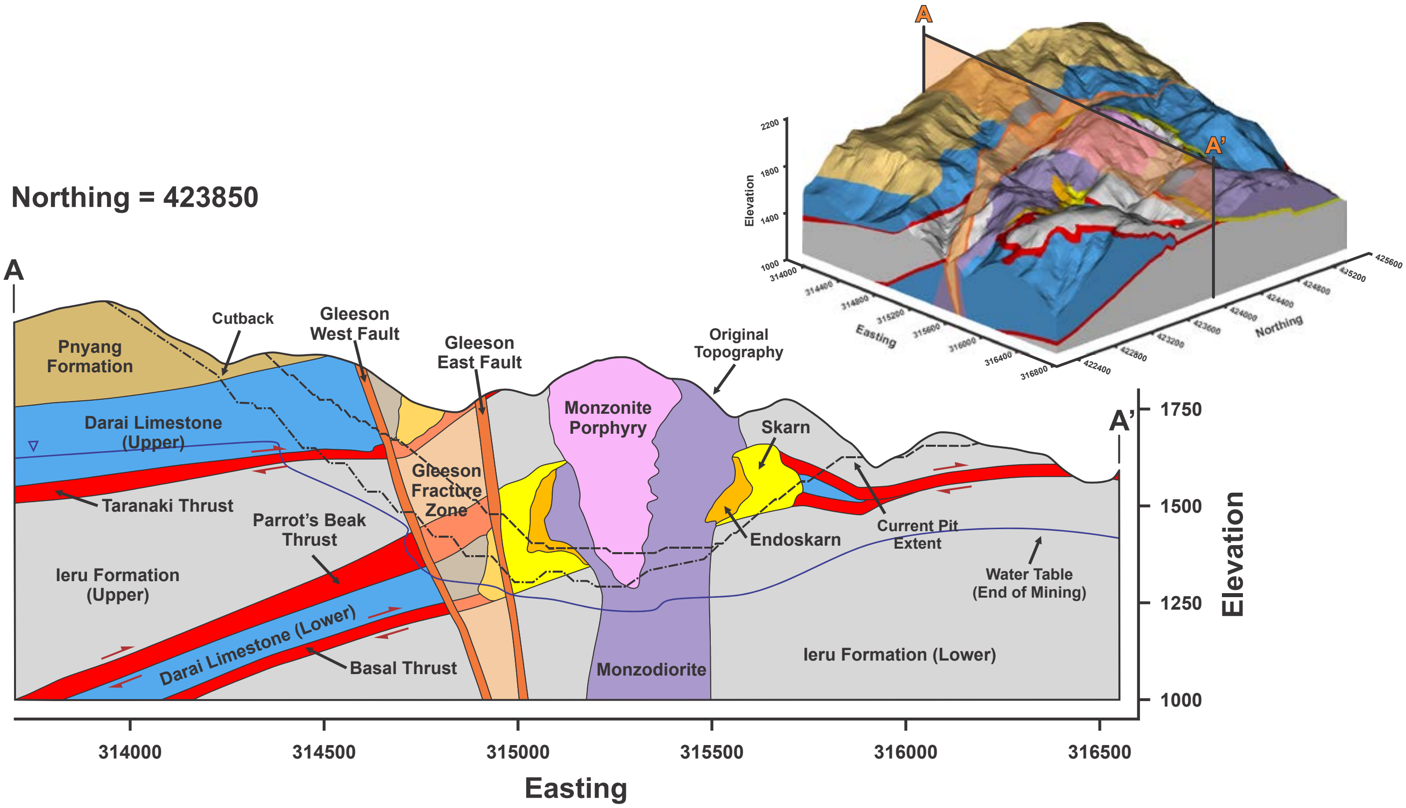

Fig. 3. Cross section through the Ok Tedi pit at a northing of 423850. Inset shows the location of the cross section relative to the pre-mining geological model.

Sedimentary units have been locally intruded by two igneous bodies, following regional thrust fault activity (de Bruyn et al. 2013). These include the Sydney Monzodiorite at the southern end of the pit and the Fubilan Monzonite Porphyry to the north (Figure 3). The Sydney Monzodiorite is the older of the two intrusions, and dates to Pliocene (2.6 Ma; Page 1975). The unit is a medium to coarse grained, dioritic intrusive body, which is generally unmineralized (de Bruyn et al. 2011). In comparison, the younger (1.1 to 1.2 Ma) Fubilan Monzonite Porphyry is mineralized and hosts the main economic mineralization, along with proximal skarnified bodies (Page 1975). The unit is a porphyritic, felsic body, which has caused local skarnification of the Darai Limestone and extensive potassic alteration of the Ieru Siltstone (Baczynski et al. 2011). Skarn units are sub-divided into four distinct units, namely: endoskarns, calc-silicate skarns, massive magnetite skarns, and massive sulphide skarns. In addition to local alteration, igneous emplacement has resulted in a slight up-doming of sedimentary strata. This has led to the sedimentary layers having a slight dip into the pit walls.

The groundwater system is dominated by a gravity driven, high recharge system, which has been compartmentalized by the Taranaki, Parrot's Beak and Basal thrust faults (Fagerlund et al. 2013). These zones result in perching and damming of internal aquifers. In total, three aquifers exist and are referred to as the Taranaki, Parrot's Beak and Basal aquifers, based on the thrust fault defining their lower surface. These thrust faults dominate the groundwater flow regime, and their slight upward doming morphology causes the majority of groundwater to flow away from the pit walls; however, minor seepage is observed on the pit wall between 40 and 100 m above the pit floor. This is enhanced by gravity driven flow mechanisms associated with the location of the Ok Tedi pit at the top of Mt. Fubilan. Hydraulic testing of sedimentary and igneous units generally indicates higher hydraulic conductivities (10^{-7} to 10^{-6} m/s) compared to fault zones (10^{-9} to 10^{-8} m/s) due to a large degree of fracture and karst development. Sub-vertical fault zones in the western pit wall are thought to further compartmentalize flow due to their high gouge content. The high recharge rates are associated with the extremely high annual rainfall (9 to 11 m) found throughout the site (Hearn 1995).

3. BOREHOLE DATA

Borehole data from the Ok Tedi mine was provided by Ok Tedi Mining Ltd. through SRK Consulting. The database included 153 boreholes, subdivided into 8,178 discrete geotechnical logging intervals. Borehole logging intervals were found to vary greatly in size, with a range of 0.01 to 64.40 m. The spatial distribution of the borehole collars is also greatly skewed towards the center of the Ok Tedi pit, coinciding with the main mineralization targets (Figure 2). Logging intervals

Table 1: GSI estimates for highly fragmented, crushed and/or decomposed zones. Ranges were approximated by SRK Consulting (Australasia) Pty Ltd. using the GSI estimation chart of Hoek et al. (2002).

Rock Description	Assigned GSI Value
Clay, clayey gravel or Fault with gouge (clay and rock fragments)	5 - 15
Sheared rock, crumbly rock, gravel or non-gouge fault	10 - 20
Intensely fractured rock or breccia, fragments <2 cm	15 - 25
Heavily fractured rock, greater than four discontinuity sets, fragments 2-5 cm	20 - 35

were characterized by on-site geotechnical staff using the Laubscher MRMR rock mass classification system and later transformed by SRK Consulting to the Bieniawski RMR_{89} system (Bieniawski 1976; Bieniawski 1989; Laubscher 1990; Jakubec and Laubscher 2000; Laubscher and Jakubec 2001).

Simulation of the rock mass behaviour was conducted using the empirical Hoek-Brown criterion (Hoek and Marinos 2007). The method is based on the assumption that rock masses fail through sliding and/or rotation of intact rock blocks and requires the definition of four parameters, namely: geological strength index (GSI), intact rock uniaxial compressive strength (σ_{ci}), material constant (m_i), and a disturbance factor (D; Hoek et al. 2002). The GSI was estimated from borehole data through conversion of RMR_{89} values. Conversion of the majority of RMR_{89} values utilized the formula (Hoek 1994):

$$GSI = RMR_{89} - 5 \quad (1)$$

However, this approach is inappropriate within highly fractured and/or decomposed intervals, as the RMR_{89} system has been shown to be unsuitable for characterizing overall rock mass behaviour in such conditions (Hoek et al. 1995; Hoek et al. 2002). To compensate for this limitation, GSI values were directly assigned to intervals described as highly fragmented, crushed and/or decomposed zones within the geotechnical database. This was conducted according to Table 1 constructed by SRK Consulting for the Ok Tedi mine site (SRK 2012). Values assigned to these highly fractured zones were treated as random variables, defined by uniform distributions within the designated GSI range. The resultant medial GSI values for each geological unit are summarized in Table 2.

Intact rock uniaxial compressive strength (UCS) was characterized directly from the Is_{50} tensile point-load test results (Table 2). Point-load estimates were chosen for two reasons. First, the dataset was large and broadly distributed throughout the study region, unlike laboratory test results which were spatially limited. Second, point-load data were collected independently from RMR_{89} estimates, unlike simple hammer tests, which exhibited an underlying bias based on the condition of the rock mass. This underlying bias is observed in the Ok Tedi dataset by an increase in the correlation coefficient between the non-declustered UCS and GSI data from 0.16 with point-load estimates to 0.61 with hammer test results.

Table 2: Medial Hoek-Brown attributes and statistics for each geotechnical domain at the Ok Tedi mine site. Data was declustered using the methodology described in Section 4.1.1 prior to characterization of the summary statistics.

Geotechnical Unit	Density (kg/m^3)	m_i	Median	
			GSI	UCS (MPa)
Monzonite Porphyry	2550	24	51	65
Monzodiorite	2550	24	40	46
Endoskarn	3250	17	46	34
Skarn	4450	17	53	76
Darai Upper	2750	10	45	69
Darai Lower	2740	10	47	65
Ieru Upper	2620	7	34	64
Ieru Lower	2620	7	53	86
Pnyang	2660	9	44	64
Thrust Fault Rock	2920	7	29	72

The material constant (m_i) is a difficult parameter to characterize as proper estimation requires detailed laboratory test results. As a result, most studies rely on published empirical estimates based on the lithology (Hoek et al. 2002). Due to this difficulty, characterization of the spatial structure for the material constant was impossible based on the current dataset. Therefore, values were kept constant throughout the geotechnical domains and were assigned based on previously published estimates for the site (Table 2; Baczynski et al. 2011).

Similar to the material constant (m_i) characterization of the disturbance factor (D) is challenging. This parameter is intended to describe the degradation of the near surface rock mass due to blasting and unloading (Hoek

2002). However, ambiguity exists within the geotechnical community in how to apply the disturbance factor (D; Little 1999; Li et al 2011; Hoek et al. 2012; Lupogo et al 2014; Styles 2015). As a result, the disturbance factor (D) was ignored throughout this study and a constant value of 0.0 used. This was conducted as the study was concerned with the relative effect of using different rock mass simulation techniques on deep-seated failure as opposed to absolute valves which consider near surface degradation.

4. METHODOLOGY

4.1. Geostatistical Simulation

Random field generation of the geological strength index (GSI) and uniaxial compressive strength (UCS) was conducted using sequential Gaussian simulation (SGS). SGS is novel within the field of open pit slope design, but has been utilized for a number of years within the geological and reservoir modelling communities (Dimitrakopoulos and Fonseca 2003; Esfanhani and Asghari 2013). The algorithm works by sequentially simulating attribute values along pseudo-random paths, while incorporating spatial co-dependencies using simple kriging routines (Journel and Huijbregts 1978; Dowd 1992; Deutsch and Journal 1998). The method used in this study involves a six step process. The following section provides a brief overview of the approach. For a more detailed description of the SGS method see Journel and Huigbregts (1978), Goovaerts (1997), or Nowak and Verly (2007).

Declustering

Prior to characterization of the spatial structure, data must first be filtered to remove spatial sampling dependencies (Prycz and Deutsch 2003). These dependencies result from the non-systematic manner of data collection and the underlying geological processes which control the studied attributes. This differs from classical statistical methods where sample independence is assumed. To remove these dependencies spatial declustering techniques are utilized, which assign differential weighting to studied attributes based on their proximity to surrounding data (Chilés and Delfiner 1999). This is done by assigning smaller weights to closely spaced data, and larger weights to widely spaced data, ensuring that closely spaced data are not over-represented within the dataset.

Three main spatial declustering algorithms exist within the literature, namely: polygonal, cell, and kriging weight declustering (Isaaks and Srivastava 1989). While all of the aforementioned methods are effective at declustering spatial data, cell declustering was chosen for de-biasing in this study due to its ease of use and ability to control the spatial scale. The method utilizes the following steps (Prycz and Deutsch 2003):

1. A grid origin is specified.
    a. Data are then overlain with a square grid based on the specified origin.
    b. The number of data in each cell (n_i) is then tabulated and a weight w_j' calculated for each as follows:

$$w_j' = \frac{1}{n_i}\frac{n}{c_i} \tag{2}$$

    where n is the total number of data, and c_i is the number of cells with data.
2. The grid origin is then shifted and step 1 repeated.
3. Finally, the weights are averaged across all of the origin simulations to give an average weight for each datum.

Multiple offsets are required to remove the cell declustering sensitivity to the grid origin. The Ok Tedi dataset was declustered using this approach with a 0.01 m offset and 1000 iterations. A 10 m^3 cell size was used to mimic the 10 m^2 cell size arrangement used in the subsequent FLAC geomechanical model.

In addition to the spatial dependencies, sampling issues exist with the borehole data due to the variable size of the geotechnical domain logging intervals. This can result in an over-representation of smaller compared to larger sampling intervals, if the data is used without any bias correction. In order to overcome this issue, borehole logs were re-sampled at a 0.01 m spacing, to prevent the under-representation of larger intervals.

In addition to cellular declustering, a moving window, averaging technique was employed to obtain average attribute values for the 10 m^2 cells subsequently used in the FLAC 2D model. The method works by sub-dividing the study region into a series of local neighborhoods of equal size and calculating summary statistics for each attribute (Isaaks and Srivastava 1989). This is similar to the declustering method and utilizes evenly spaced, square windows generated based on a designated grid origin. The final result ensures that data are averaged to the same scale as the final geomechanical suimulation model, limiting the influence of small discrete anomalies.

Detrending

Following cell declustering it is important to filter the large-scale spatial trends due to their poor reproducibility by the SGS process. This is due to the fact that the SGS technique reproduces random phenomena assuming data conforms to the first-order stationary assumption (Journel and Huigbregts 1978). This assumption is referred to as the intrinsic hypothesis and states that both the mean and variance are dependent strictly on the data separation distance and not the location of the data (Matheron 1963). If data do not conform to this assumption due to systematic trends, then trends must be defined and removed/filtered prior to conducting SGS (Deutsch 2002).

Identification of spatial trends is conducted through exploratory spatial data analysis techniques, including: semivariogram analysis, average grade profiles, and ordinary kriging with a high nugget effect (Vieira et al. 2010). The use of average grade profiles is the simplest and often first means of trend identification. It involves the examination of averaged data along one, two or three dimensional profiles (Isaaks and Srivastava 1989; Deutsch 2002). Once identified, trends can then be characterized using moving average techniques, kernel estimation and/or ordinary kriging with a high nugget effect (Hallin et al. 2004; Nowak and Verly 2007).

Following identification and characterization, the most common way to deal with trends is to first remove them, then simulate the residuals, and finally add the trend back to the simulated results (Vieira et al. 1983; Vieira et al. 2002; Blackmore et al. 2003; Jenson et al. 2006). This filtering process commonly employs a number of techniques including: subdividing the data into a series of domains (Deutsch 2002), linear regression with a correlated variable (Phillips et al. 1992) and polynomial trend analysis (Vieira et al. 2010).

Analysis of the spatial trends within the Ok Tedi dataset identified the influence of the Gleeson fracture zone, which affected GSI estimates from all geotechnical units within the western pit wall. To remove this trend, data were filtered using a constant ratio of 0.81, which is equal to the average decrease of GSI values within the zone. Residuals obtained from the filtering process were used for the remainder of the SGS process and the trend added back following simulation.

Normal Score(Gaussian) Transformation

The SGS algorithm is based on an assumed multi-Gaussian system, where the spatial variance arises from random processes acting on a stationary mean (Goovaerts 1997). In order to satisfy this assumption, one commonly utilized method involves a Gaussian transformation of the data (Journel and Huijbregts 1978). This is conducted to ensure data adhere to a normal distribution. Under the assumption of a spatially constant trend, the process involves assigning a standard normal score to each datum such that the cumulative frequencies of both the normal score and attribute are identical (Chilés and Delfiner 1999). This

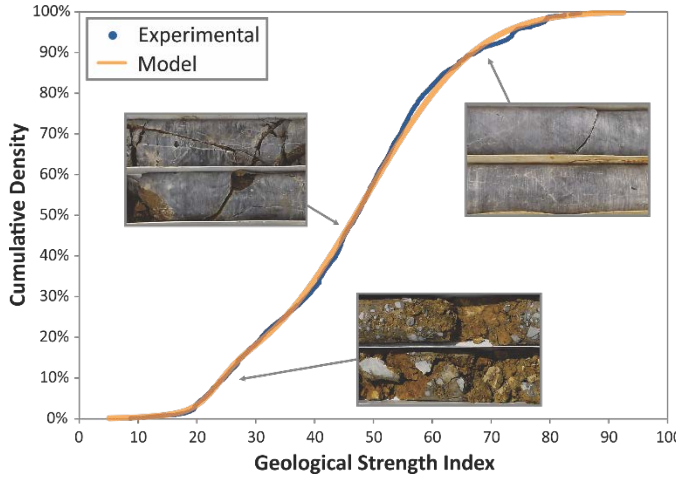

Fig. 4. GSI data were converted to normal score space using a cumulative frequency plot. Normal scores were selected based on the matching cumulative frequencies between the data and a normal distribution. Examples are from the Upper Darai Limestone.

transformation process is conducted either graphically from the modelled cumulative density function (CDF) or by defining a transformation function using a polynomial expansion (Castrignanò et al. 2009).

The Ok Tedi data were transformed by first assigning distribution models to the studied attributes prior to the normal score transformation. This was done to smooth the data and have the transformation better reflect the likely underlying sample distribution. Bimodal normal and Weibull distributions were used for the GSI and UCS, respectively. Standard normal score values were then assigned to datum based on a piecewise approximation of the cumulative frequencies from the modelled CDFs (Figure 4). A back-transformation function was also constructed allowing for conversion of modelled normal scores back to GSI and UCS values following SGS simulation.

Correlogram Analysis

Accurate characterization of the underlying spatial structures is the foundation of any geostatistical analysis involving kriging and/or SGS (Clark 1979; Isaaks and Srivastava 1989). The standard method within geostatistics used to characterize this structure is semivariogram analysis which measures the spatial dissimilarly vs. distance. Since it is assumed that closely spaced data are more closely related than distant, semivariograms should display increased dissimilarity with distance, until the point at which no obvious correlation exists between data values. At this point, the semivariogram reaches a sill that is comparable to the sample variance. Classic geostatistical analysis within the mining industry typically utilizes semivariograms; however, alternative methods of modelling spatial dependency exist (i.e. covariograms and correlograms).

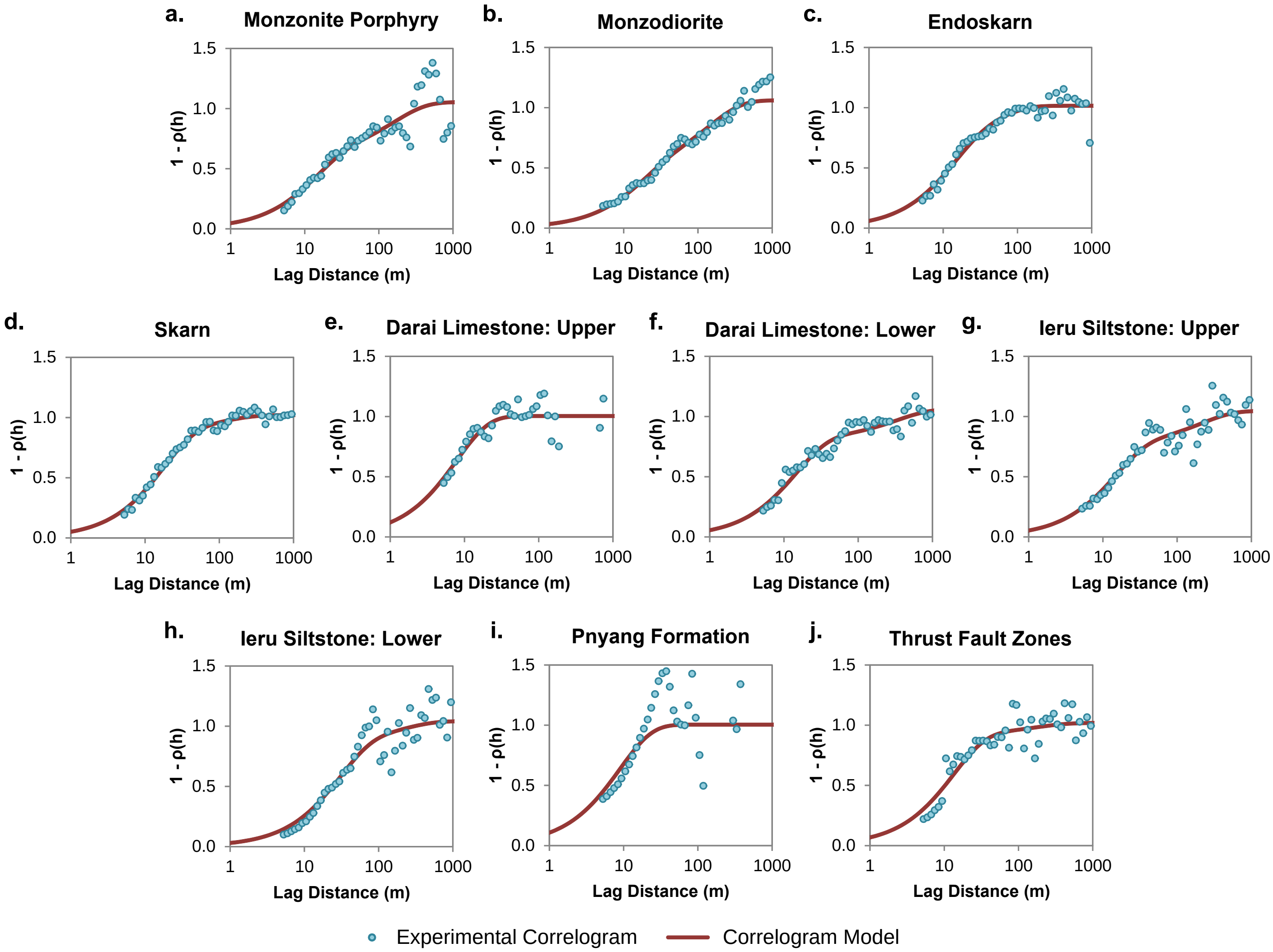

Fig. 5. Normal score correlograms for geological strength index (GSI).

Srivastava and Parker (1989) demonstrated that correlograms may be more robust than semivariograms in the presence of preferentially sampled data. The use of correlograms/covariograms also allows for greater continuity between the statistical modelling and geostatistical simulation as the kriging/SGS process requires the direct input of covariance vs. distance models (Journel and Huijbregts 1978). For these reasons, spatial analysis at Ok Tedi was conducted utilizing correlograms.

Correlogram analysis was conducted by first calculating average correlation coefficients vs. distance. The algorithm incorporated declustered weights using the following formula:

$$\rho(h) = \frac{1}{\sum\sum w_i w_j} \sum\sum w_i Z_i w_j Z_j \qquad (3)$$

where Z_i and Z_j are the normal score values, w_i and w_j are the declustered weights and $\rho(h)$ is the correlation coefficient at the specified lag distance. Lags were calculated in a logarithmic space, to give greater refinement of average correlation coefficients at shorter lag distances.

Correlogram models were then fit to the experimental data for the GSI and UCS using least squared regression techniques. GSI continuity was modelled with two nested structure models with zero nugget effect, while UCS continuity was modelled using an exponential model and relatively high nugget effect (Table 3; Figure 5 and 6). Models were constrained to reproduce a dispersion variance of 1.0 within the simulation area (Journel and Huijbregts 1978).

Sequential Gaussian Simulation

Inherent heterogeneities within the Ok Tedi rock mass system were simulated using the sequential Gaussian simulation (SGS) method (Dowd 1992; Nowak and Verly 2004; Leuangthong et al. 2011). The method works by sequentially simulating a series of normal scores at specified grid nodes using a random walk process coupled with simple kriging routines (Vann et al. 2002). The method was chosen due to its ability to reproduce continuous random variables, while also

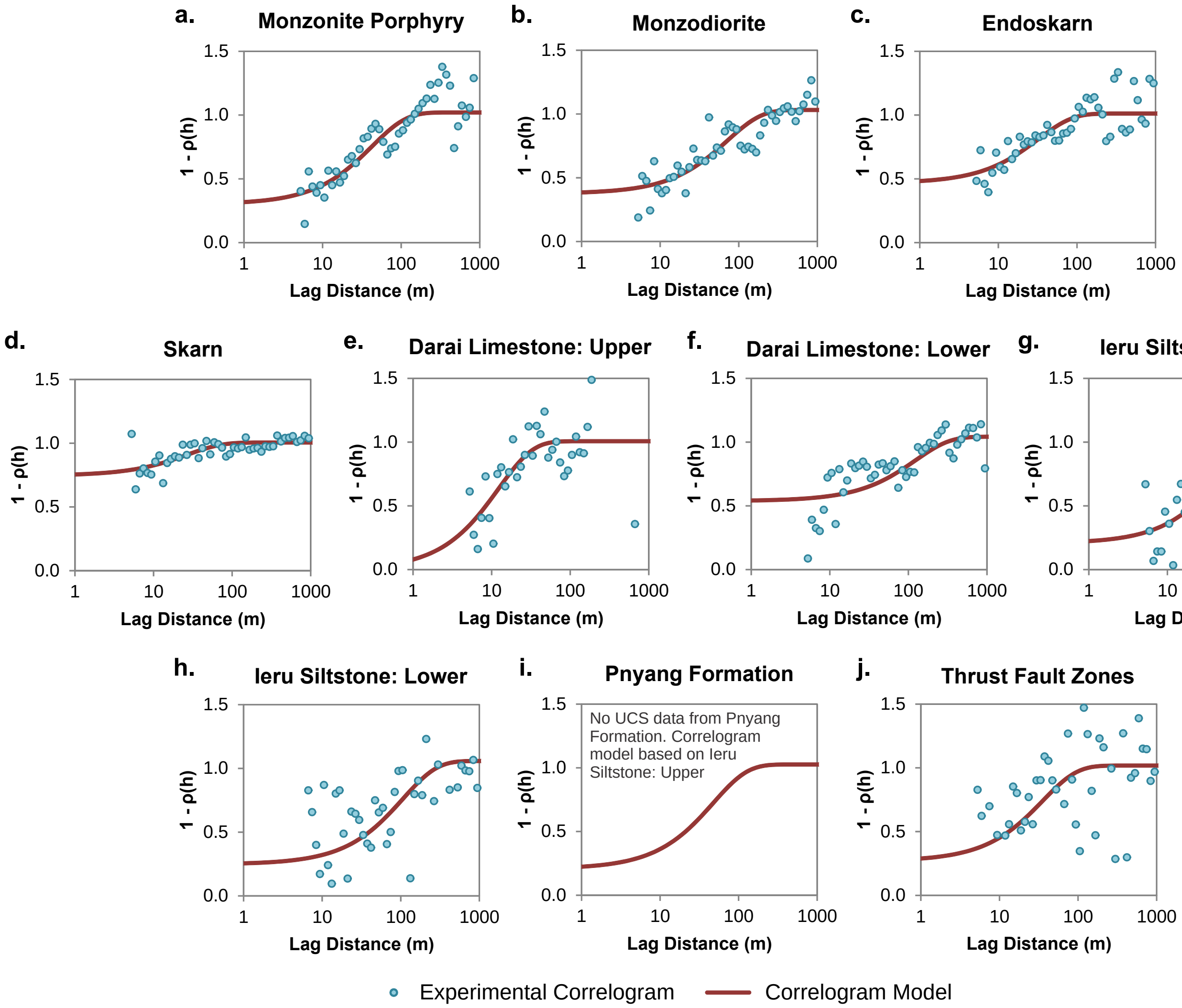

Fig. 6. Normal score correlograms for uniaxial compressive strength (UCS).

taking into consideration the underlying spatial structure. The basic steps in the algorithm are as follows (Journel and Huijbregts 1978):

1. Generate a random walk sequence through the simulation grid nodes.
2. Visit the first node in the sequence and simulate a value by a random draw from a conditional distribution derived from simple kriging.
3. The simulated value becomes part of a conditioning set.
4. Visit the next node in the sequence and simulate the studied attribute using both original and simulated values for conditioning.
5. Repeat step 4 until all nodes have been visited.

While the method preserves the spatial structure defined by the semivariogram, there are two main possible limitations of the method that need to be taken into consideration (Vann et al. 2002). First, the simulation area must be greater than the range of the defined spatial dependency model, otherwise the full spatial structure of the model will not be preserved by the simulation. Next, an adequate number of neighboring data points must be used during conditioning, or the simulation will heavily favor the short lag trend in the spatial model.

SGS was conducted within this study using FISH routines written to conduct the simulation directly within the software package FLAC (Figure 7; Itasca 2011). Simulations were conducted in normal-score space and back-transformed to parameter space following geostatistical simulation, with the previously removed Gleeson fracture zone trend added back to the results. GSI and UCS simulations were conducted independently due to the poor correlation coefficient between the two parameters ($r = 0.19$).

4.2. Geomechanical Simulation

Geomechanical simulation was conducted using the Itasca software Fast Lagrangian Analysis of Continua (FLAC; Itasca 2011). FLAC is a two-dimensional, finite-difference simulation package, which simulates continuum type behaviour using predefined constitutive criterion models (i.e. Mohr-Coulomb, Mohr Ubiquitous-

Joint, Hoek-Brown, etc.). During simulation, the material undergoes linear elastic behaviour until its yield point is reached, at which point it behaves as a plastic material, whose properties are defined by the specified constitutive models.

Geomechanical simulations of the Ok Tedi pit involved a 2D east-west cross-section through the center of the pit (Figure 2; Figure 3). Staging was not conducted as FLAC modelling suggested that given perfectly-plastic behaviour there is very little difference between staged and non-staged models at the Ok Ted mine site. Results from the FLAC modelling indicated a factor of safety of 1.79 and 1.78 for the staged and non-staged models, given medium-value deterministic simulations. As a result, increased computational efficiency was achieved by ignoring staging and running models using the final excavation stage of the proposed west wall cutback.

Failure criterion within the FLAC simulations utilized the integrated, modified Hoek-Brown criterion (Hoek et al. 2002; Itasca 2011). The criterion is based on the general non-linear Hoek-Brown stress relationship:

$$\sigma_1 = \sigma_3 + \sigma_{ci}\left(\frac{m_b}{\sigma_{ci}} + s\right)^a \quad (4)$$

where σ_{ci} is the unconfined compressive strength, m_b, s and a are material constants related to the Geological Strength Index (GSI), damage parameter (D), intact rock constant (m_i) and intact rock uniaxial compressive strength (UCS) (Hoek et al. 2002). The criterion is incorporated into the FLAC simulation code using a linear approximation obtained by fitting a tangential Mohr-Coulomb envelope to the failure criterion. The approximated envelope is extended for tensile failure through a combination of curve matching the tangential Mohr-Coulomb envelope to the Hoek-Brown at $\sigma_3 = 0$ and a tensile cutoff of $\sigma_3 = -s\sigma_{ci}/m_b$. Dilation mechanics during plastic strain are simulated using a dilation angle (ψ_c) estimated from the linear approximation provided by Hoek et al. (1997):

$$\sigma_1 = \sigma_3 + \sigma_{ci}\left(\frac{m_b}{\sigma_{ci}} + s\right)^a \quad (5)$$

One limitation of the Hoek-Brown criterion is its inability to characterize low GSI conditions, where failure ceases to be controlled by translation and rotation of individual blocks (Hoek et al. 2002; Carter et al. 2007). At these low GSI values (UCS_{ir} < 0.5 MPa) materials typically behave more as a “soil-like” substance, with behaviour best described by the Mohr-Coulomb strength criterion (Carvalho et al. 2007). The rock mass only begins to behave as a Hoek-Brown substance after the UCS_{ir} exceeds 10-15 MPa (Brown 2008). An empirically derived criterion used to describe the transition between these two extremes was proposed by Carter et al. (2008):

$$f_T(\sigma_{ci})\begin{cases} 1, & \sigma_{ci} \leq 0.5\ MPa \\ e^{\frac{-(GSI-0.5)^2}{25}}, & \sigma_{ci} > 0.5\ MPa \end{cases} \quad (6)$$

which facilitates the transition from linear soil-like behaviour to non-linear rock mass type behaviour. This relationship was incorporated into the FLAC

Table 3: Normal score variogram constraints for the Ok Tedi dataset.

Geotechincal Unit	GSI				UCS (MPa)		
	Exponential Model I		Exponential Model II		Nugget	Exponential Model	
	Sill	Range (m)	Sill	Range (m)		Sill	Range (m)
Monzonite Porphyry	0.61	41	0.44	489	0.30	0.72	128
Monzodiorite	0.49	49	0.57	434	0.38	0.66	214
Endoskarn	0.69	38	0.32	149	0.47	0.55	97
Skarn	0.88	52	0.14	335	0.74	0.26	81
Darai Upper	1.00	24	-	-	0.00	1.01	37
Darai Lower	0.81	43	0.25	1000	0.54	0.50	369
Ieru Upper	0.76	43	0.29	630	0.21	0.82	143
Ieru Lower	0.86	88	0.18	614	0.25	0.81	318
Pnyang	1.00	27	-	-	0.21	0.82	143
Thrust Fault Rock	0.92	40	0.10	513	0.27	0.75	107

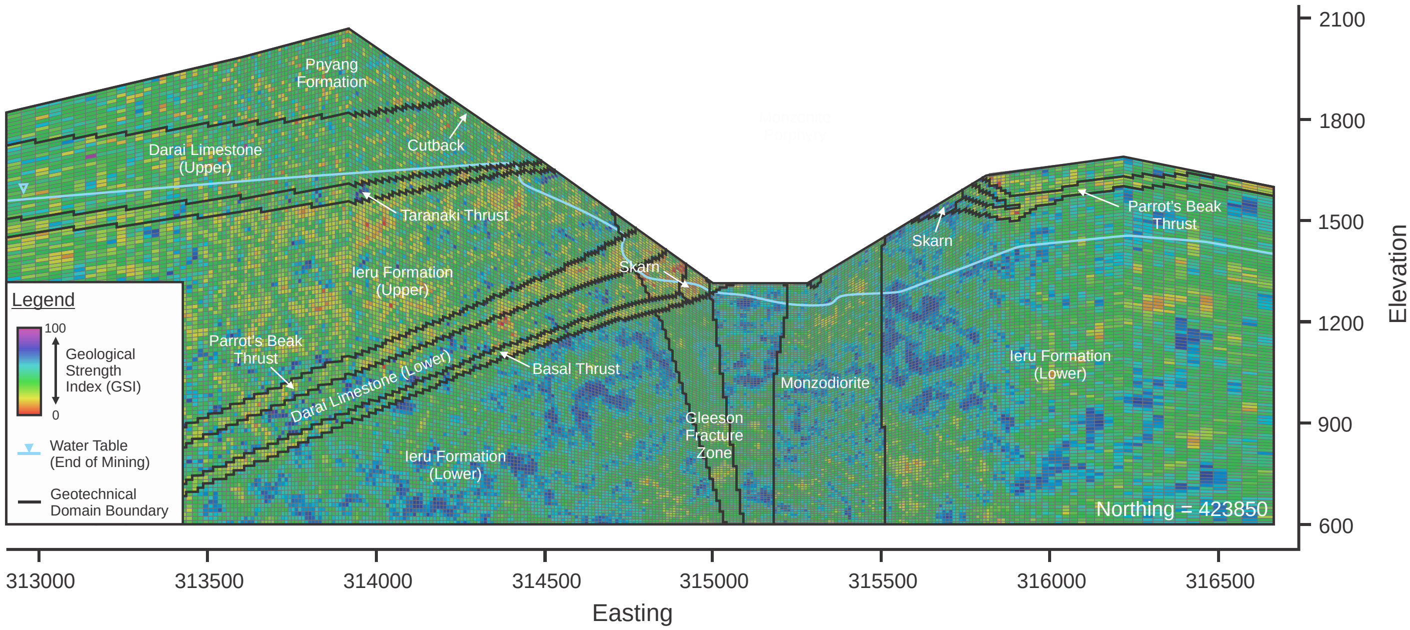

Fig. 7. Single realization of the GSI attribute for end-of-mining conditions generated using the SGS method described herein.

simulations, by extending the modified Hoek-Brown criterion through a user-written FISH function.

Spatial heterogeneity was incorporated into simulations using the SGS process. This ensured that unique GSI and UCS values were associated to each individual grid node. These attributes were used, along with domain constant m_i values, to assign unique Hoek-Brown a, s, and m_b parameters to each individual node. Disturbance zone (D) factors were ignored in the simulations as the purpose was to explore deep-seated failure.

Elastic moduli and Poisson's ratio were estimated dynamically from the randomly generated GSI and UCS values. The elastic modulus (E) was estimated using the equation (Hoek et al. 2002):

$$E\ (GPa) = \begin{cases} \left(1-\frac{D}{2}\right)\sqrt{\frac{\sigma_{ci}}{100}}\ 10^{\frac{GSI-10}{40}}, & \sigma_{ci} \leq 100\ MPa \\ \left(1-\frac{D}{2}\right)\ 10^{\frac{GSI-10}{40}}, & \sigma_{ci} > 100\ MPa \end{cases} \tag{7}$$

while, the Poisson's ratio (v) was estimated from (Hoek et al. 1995):

$$v = 0.32 - 1.5\frac{GSI}{1000} \tag{8}$$

Groundwater conditions were incorporated into FLAC simulations based on groundwater modelling of the Ok Tedi system by Fagerlund et al. (2013) using the DHI-WASY software FEFLOW (DHI-WASY 2013). The flow model was designed to estimate the pore pressure distribution following the west wall cutback, through a transient 5-year groundwater simulation from current to proposed pit conditions.

Models were assessed by conducting a shear strength reduction (SSR) analysis once steady-state conditions had been achieved (Mattsui & San 1992; Dawson et al. 1999; Diederichs et al. 2007). The general concept of a SSR analysis is to systematically reduce the shear strength envelope of a material until deformations are considered to be unacceptably large or solutions do no converge. The factor by which the shear strength is reduced to reach this critical level the critical shear stress reduction factor (SRF) and is equivalent to the factor of safety in classical limit equilibrium analysis (Hammah et al. 2005; Hammah et al. 2006). Simulations employed Monte Carlo sampling techniques, which allowed for derivation of the SRF distribution and estimation of the probability of failure. Simulations were conducted using a constant mesh geometry. Runtimes were approximately 8 days per 100 models, for a 3.4 GHz PC with 16 GB of RAM.

The basic formulation of FLAC is as a plane strain model, which simplifies the full three-dimensional slope stability problem as infinitely long two-dimensional features (Itasca 2011). Various studies have shown that this simplification can result in reduced SRF estimates compared to full 3D analyses, as plane strain conditions increase overall kinematic freedom within 2D models (Cavounidis 1987; Chugh 2003; Albataineh 2006; Cala et al., 2006, Jiang et al., 2008). Despite these limitations two-dimensional analysis is still widely used throughout geotechnical mine design as a simplification of three-dimensional behaviour (Hormazabal et al. 2013; Abrahams et al. 2015; Wen et al. 2015; Wolter et al. 2015; Argumedo et al. 2016; Tuckey et al. 2016). While geotechnical analysis in this study has applied 2D simplifications of the Ok Tedi pit, the same geostatistical methodology would also be applicable for full 3D analysis.

4.3. Critical Area Estimation

Recent advances in mine design practice have focused on an increased drive towards deeper and more complex designs (Read and Stacey 2009). This has forced geotechnical engineers to consider methods other than traditional deterministic techniques, which can characterize the inherent uncertainty associated with increased mine complexity. As a result, a renewed interest exists within the field towards more probabilistic and/or risks based practices (Steffen 1997; Terbrugge et al. 2006; Steffen and Contreras 2007; Steffen et al. 2008). This paradigm shift towards an increased focus on project risks requires an appreciation for both the probability of an unacceptable event occurring, as well as the associated consequences of the event (Yoe 2011). The first stage in understanding these consequences requires the ability to assess the size of a potential failure.

Our study applied a novel approach to estimate the failure size through the use of network analysis based techniques. The approach estimates the critical failure area through minimum distance analysis of shear strain rates obtained from numerical simulation. The first stage of the analysis involved inverting the shear strain rate values to construct an inverse shear strain rate matrix. Dijkstra's (1959) algorithm was then used to estimate minimum paths through this matrix, for each of the simulations, between the pit face and rear slope crest (Figure 8). This was conducted for each boundary node along the toe and slope of the modelled open pit. Minimum paths were then assessed based on average inverse shear strain rates, with the lowest average rate path determined to be the critical failure path. Summary statistics were calculated for the GSI and UCS along the identified path, which gave an indication of the critical shear strength within the models. Critical paths were also used to estimate the size of potential failures, by calculating the total area between the critical failure surface and slope face.

Critical path density plots were constructed from the estimated failure path results to give an indication of the critical failure surface distribution. This involved estimating nodal intersection probabilities for each of the FLAC grid cells, measured as the probability of a critical path intersecting a specified node. For example, if five critical paths out of the total of 100 Monte Carlo simulations intersected a grid node, the intersection probability at that node would be 0.05. Intersection results were then exported to ArcGIS and ordinary kriging techniques utilized to interpolate a failure path density. The resultant kriged surface gave an indication of the distribution of failure paths within the FLAC simulations.

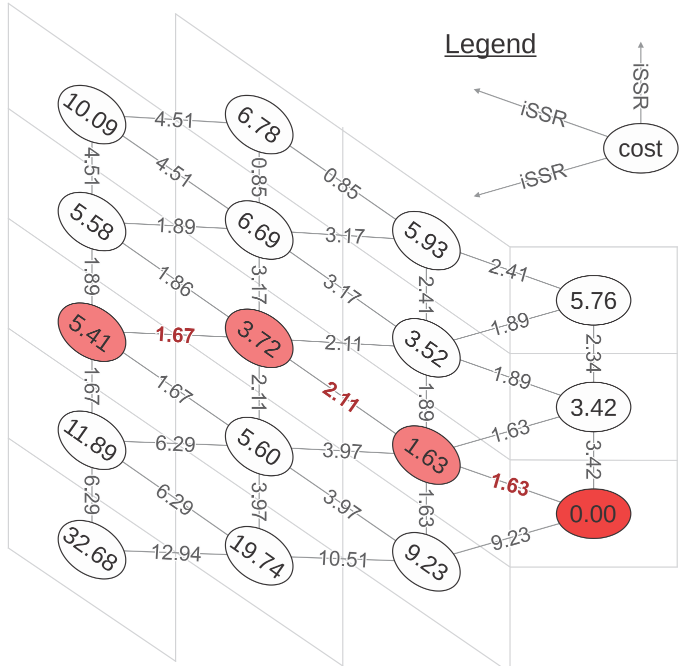

Fig. 8. Critical failure paths were identified using minimum distance analysis. The methodology utilized Dijkstra's (1959) shortest path algorithm.

4.4. Statistical Up-Scaling

One of the difficulties in utilizing the geostatistical simulation technique is the data intensive analysis that must be conducted to characterize and simulate the spatial structure. While this can be considered an ideal to strive for, it is not always practical or possible due to both time and data constraints. Therefore, a number of researchers have proposed the use of critical path algorithms to up-scale attribute distributions from the borehole to domain scale (Glynn et al. 1978; Glynn 1979; Shair 1981; Einstein et al. 1983; Baczynski 2008). These algorithms work by identifying critical paths through synthetic rock material, using either minimum distance (O'Reilly 1980) or random step-path generation (Baczynski 2000) techniques. Strength attributes are then summarized for the paths and incorporated into geomechanical software packages. To test this general methodology, a software package was developed to quickly refine geotechnical domain statistics based on a preliminary understanding of the local heterogeneity. The program uses the following steps:

1. A two dimensional simulation area is defined by a n by $n/2$ matrix, where n is equal to the user-specified failure length divided by a simulation cell size.
2. GSI and UCS values are assigned to the simulation area using the sequential Gaussian simulation algorithm described in Section 4.1.5. This requires a user specified variogram model for both geotechnical attributes.

3. Hoek's global rock mass strength values (σ'_{cm}) are then assigned to each node based on the simulated GSI and UCS values, and a user-specified m_i attribute, using the equation (Hoek and Brown 1997):

$$\sigma'_{cm} = \sigma_{ci} \frac{(m_b + 4s - a(m_b - 8s)) \left(\frac{m_b}{4} + s\right)^{a-1}}{2(1+a)(2+a)} \quad (9)$$

where a, s and m_b are the Hoek-Brown constants, and σ_{ci} is the uniaxial compressive strength of intact rock.

4. Dijkstra's (1959) algorithm is then used to calculate the critical paths through the simulation area, based on a minimum distance analysis of global rock mass strength values.

5. GSI and UCS values from nodes along the critical path are then averaged to give an indication of the overall strength of the weakest path through the simulation.

Up-scaled GSI and UCS values are then incorporated into geomechanical simulations and assigned uniformly across geotechnical domains.

The proposed algorithm was used to conduct three separate simulations. This includes:

- The simulation of each geotechnical unit independently, and the GSI and UCS statistics summarized accordingly.
- The co-simulation of all geotechnical units into a single large matrix, which was then used to find an overall weakest path. GSI and UCS values were then averaged for each of the geotechnical units, allowing for co-dependencies to be taken into consideration during rock mass failure.
- Finally, co-simulation was coupled with an estimation of the step-path scale roughness (θ_{rough}) using the formula:

$$\theta_{rough} = \operatorname{atan}\left(\frac{L_{vertical}}{L_{horizontal}}\right) \quad (10)$$

where $L_{vertical}$ and $L_{horizontal}$ are the total length of the step-path in the vertical and horizontal directions. Angles were then incorporated into geomechanical simulations using a dilation angle, to simulate the volumetric change that must occur in response to step-path failure. This methodology is a simplification of reality and assumes that the failure direction is equal to the average step-path direction (Baczynski 2014). Unfortunately, no alternative, robust methodologies exist within the geotechnical literature to estimate and simulate this large, slope-scale roughness.

5. SIMULATION RESULTS

This section provides an overview of the results obtained from the geomechanical modelling. Simulations employed Monte Carlo techniques with a minimum of 100 trials conducted in each set of simulations. This was done in order to obtain a distribution of the SRF, with reasonable estimates of the mean and standard deviation. The number of trials corresponds with a stabilization of the mean and standard deviation, within a reasonable simulation timeframe (Figure 9). On average, it is observed that the number of trials required for

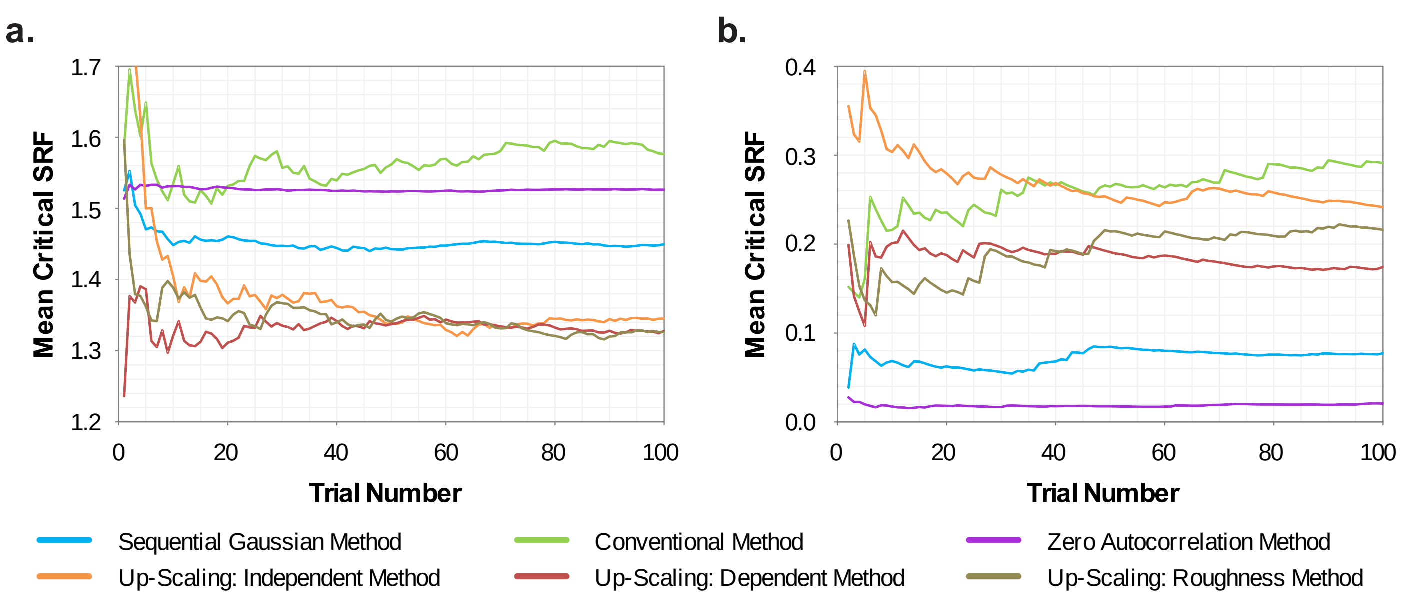

Fig. 9. Plots of the running average a mean and b standard deviation in SRF results. Results suggest that the required number of simulations is inversely proportional to the degree of spatial autocorrelation.

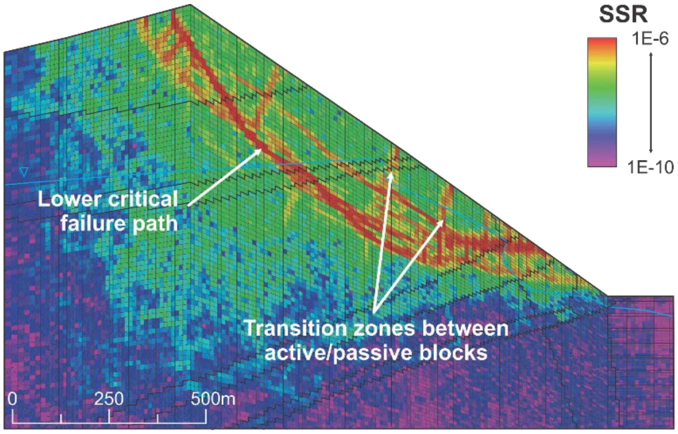

Fig. 10. Development of shear bands between the active and passive blocks is observed in the FLAC model. This behaviour helps to facilitate movement of material along the lower critical failure surface.

stabilization of the normal distribution statistics is inversely related to the degree of spatial autocorrelation within the models.

5.1. *General Observations*

Incorporation of spatial heterogeneity into continuum simulations resulted in a fundamental change in the model behaviour. Instead of models being able to indiscriminately fail anywhere in the rock mass, heterogeneous models restricted failure to the weakest areas, resulting in step-path geometries (Figure 10). This behavioural shift resulted in a reduction of the SRF from 1.63 in the deterministic simulation, to an average of 1.45 within the SGS simulations (Figure 11). Critical path analysis further confirms that damage is preferential to the weakest areas of the rock mass in SGS models, with an average reduction of 14% and 32% in the critical path GSI and UCS compared to average values in the

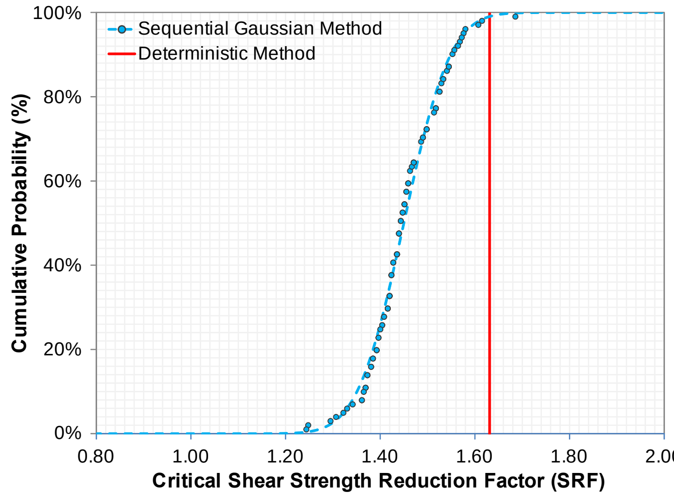

Fig. 11. Cumulative density plot comparing the SGS method with a standard deterministic analysis. The deterministic analysis utilized homogeneous units, with strength attributes defined using medial value statistics (SRF = 1.63). SGS modelling conforms to a normal distribution, with a mean SRF of 1.45 with a standard deviation of 0.08.

western pit wall (Figure 12). These results are consistent with previous research into the effects of heterogeneity which have observed this preferential failure behaviour, and reduction in strength compared to deterministic simulations (Griffiths and Fenton 2000; Hicks and Samy 2002; Lorig 2009; Jefferies et al. 2008; Srivastava 2012).

Previous two-dimensional, geomechanical simulation studies from the central Ok Tedi pit area estimated safety factors between 1.25 and 1.40, based on Slide (Rocscience 2014), GALENA (Clover 2010), and UDEC (Itasca 2014) modelling (Baczynski et al. 2011). Comparison of this previous work with FLAC simulations suggests relatively good agreement between the various analyses, given the varying methods for

Table 4: Variation in failure area and length statistics provide an estimate of the overall deep vs. shallow seated nature of the estimated failure surfaces. Trends in the coefficient of variation within the failure area and length statistics can be used as a quantitative estimate of the overall dispersion in failure path results.

Model Simulation Technique	Failure Length (m)		Failure Area (m^2)	
	Mean	Coefficient of Variation (%)	Mean	Coefficient of Variation (%)
Sequential Gaussian Simulation	1453.6	10.8	2.29 x 10^5	34.2
Conventional Probabilistic	1431.3	19.1	2.29 x 10^5	41.1
No Spatial Autocorrelation	1403.4	4.1	2.13 x 10^5	16.0
Up-Scaling: Independent	1416.3	23.5	2.33 x 10^5	44.0
Up-Scaling: Dependent	1459.7	12.7	2.54 x 10^5	28.8
Up-Scaling: Roughness	1508.8	14.1	2.66 x 10^5	29.4

deriving rock mass strengths. The slightly higher deterministic SRF estimated from FLAC simulations can be attributed to the use of medial-value rock mass strengths compared to *"best-engineering judgement"* used in previous work.

5.2. Critical Path and Area Estimates

SGS model critical path estimates suggest that failure is generally quasi-circular in nature, with daylighting typically occurring at the toe of the slope (Figure 13). Strain concentration in the toe is the result of a weaker rock mass within the Gleeson fracture zone, compared to surrounding rock. However, a few exceptions to this failure geometry exist, where stronger than average properties are simulated within the fracture zone, resulting in either deep-seated rotational or shallow pit wall failures. Deep-seated rotation failures are found to exhibit vertical shear banding between active and passive blocks, further facilitating quasi-rotational failure (Figure 10). Failure paths are found to concentrate exclusively within the western pit wall, due to the increased slope heights and on average lower GSI values compared to the east wall (Figure 7). Failure area estimates suggest a mean area of 2.3 x 10^5 m^2, with a standard deviation of 7.8 x 10^4 m^2 (coefficient of variation = 34%; Figure 11; Table 4).

With the exception of the Gleeson fracture zone, failure does not appear to be substantially dominated by any other geological units (Figure 13). This indiscriminate nature of failure development can be attributed to the sub-horizontal orientation of sedimentary layering dipping away from pit walls, and the similar geotechnical characteristics between units (Table 2). In addition, thrust zones do not appear to exhibit a major influence on the failure mechanism, due to their westward dip away from the pit wall.

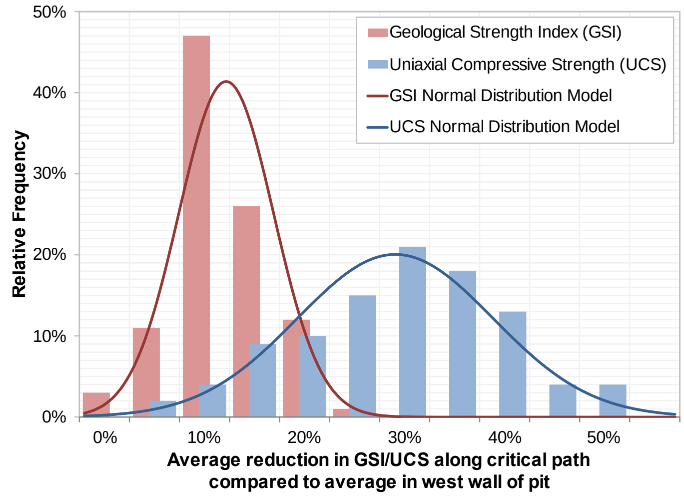

Fig. 12. GSI and UCS attributes are found to be reduced along the critical failure path compared to west wall averages. A mean reduction of 14 and 32% was found in the GSI and UCS, respectively

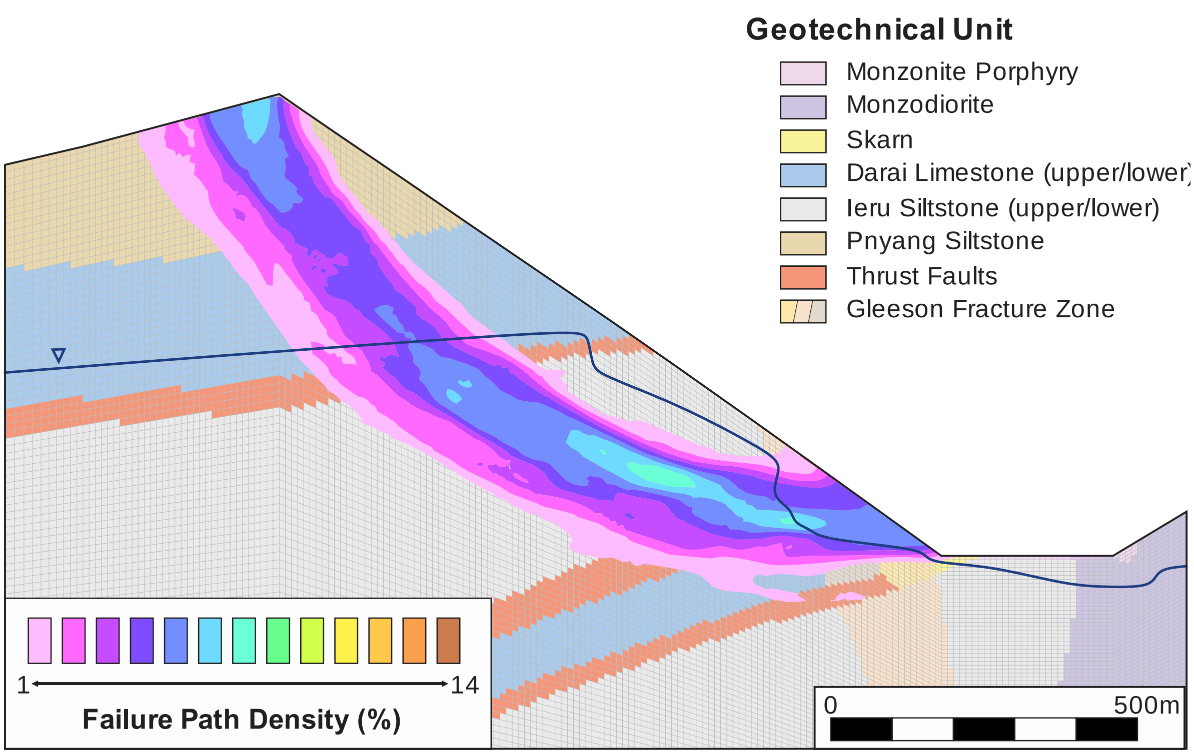

Fig. 13. Distribution of critical failure surfaces from the SGS simulations. Daylighting is concentrated within the Gleeson fracture zone. The failure area is estimated to be 2.29 x 10^5 m^2 with a standard deviation of 7.82 x 10^4 m^2, while the failure length has a mean of 1,454 m with a standard deviation of 157 m.

5.3. Conventional Probabilistic Techniques

Conventional probabilistic techniques assume that geotechnical units are spatially homogenous, with attributes defined by single random variables (Read and Stacey 2009). In order to compare this approach with the SGS method, a series of conventional geomechanical simulations were conducted. Models utilized declustered domain statistics (Section 4.1.1). Simulations were conducted using Monte Carlo techniques, whereby, two standard normal deviates were randomly selected for each of the geotechnical units (GIS and UCS). Normal score transformation functions were then used to obtain GSI and UCS attributes from the deviates. Simulated values were then assigned uniformly to all cells within the geotechnical domain. All other geotechnical attributes (e.g. m_i) were kept constant during the simulations (Table 2).

Simulation results suggest that the conventional approach over-predicts both the SRF mean and variance compared to the SGS method (Figure 14). This is observed by an increase in both the mean SRF (1.54 vs. 1.45), and standard deviation (0.29 vs. 0.08), resulting in an over-prediction of the probability of unsatisfactory performance by nearly seven orders of magnitude. Although a conservative probability was estimated while using the conventional approach, this behaviour cannot always be assumed for all studies. For example, while the conventional approach over-estimated the variance, increasing the spread of the distribution and leading to an overly conservative design, it also over-estimated the mean leading to an upward translation of the critical SRF distribution, promoting an optimistic design. This

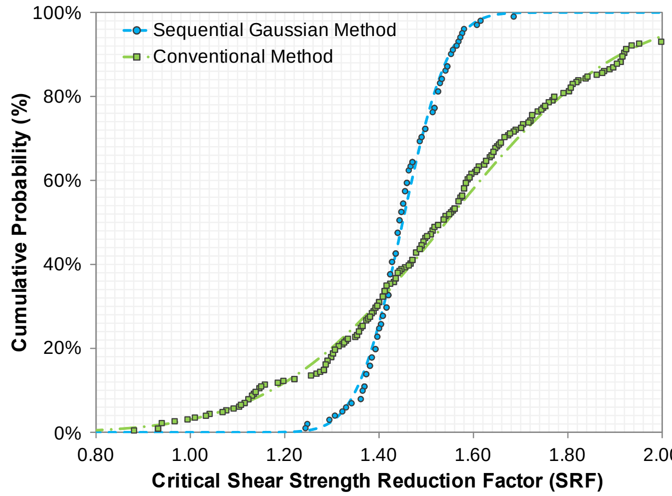

Fig. 14. Comparison of SRF results for both the SGS and conventional approaches to geotechnical slope design. The simulation results suggest that the conventional probabilistic approach overestimates both the mean SRF (1.45 vs. 1.54) and standard deviation (0.08 vs. 0.29) compared to the SGS method.

results from the fact that the conventional approach forces failure through whatever material is simulated; whereas, SGS models preferentially allow failure within the weakest areas of the rock mass, ignoring the stronger areas of the simulations. A summary of the results and hypothesis testing to ensure independence between the distributions is provided in Table 5.

A comparison of the critical area estimates between the conventional and SGS methods indicates the same means (2.29 x 10^5 m^2) but different coefficients of variation (41% vs. 34%; Figure 15; Table 4). This

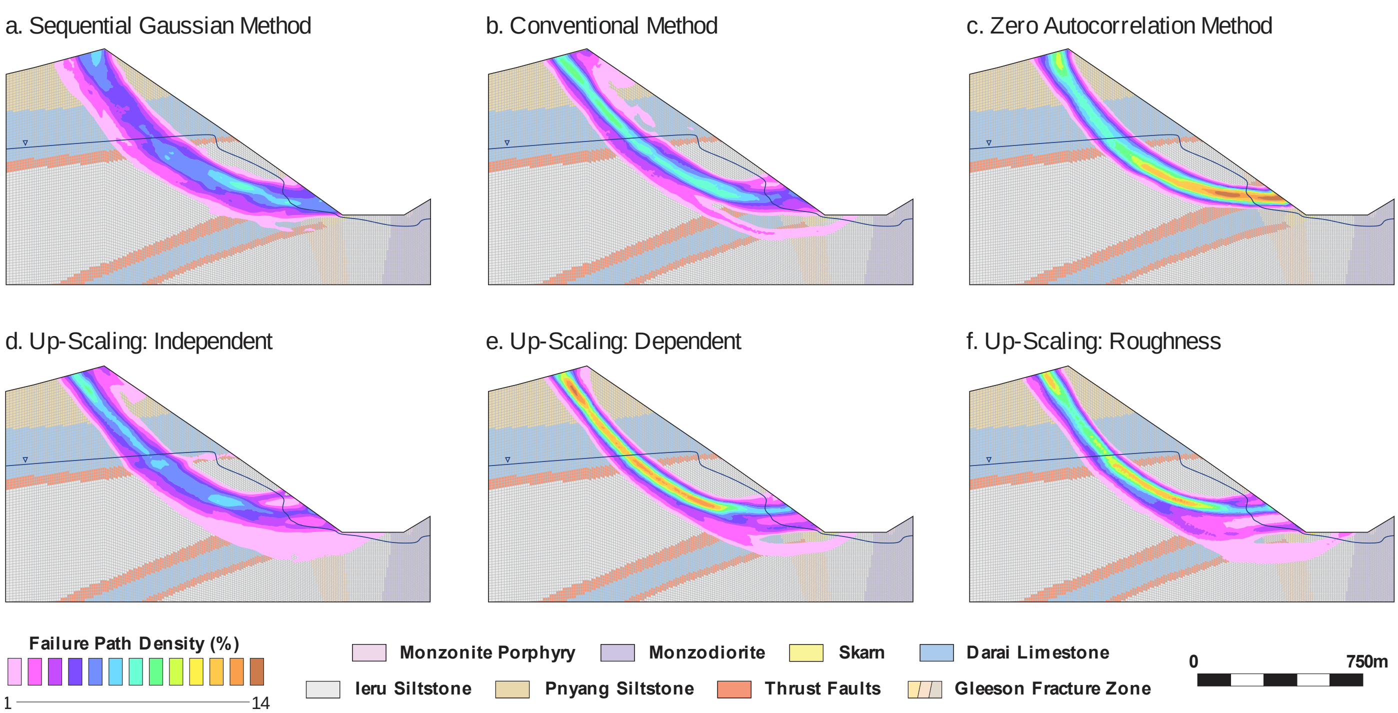

Fig. 15. Comparison of critical failure path distributions for different modelling approaches.

Table 5: Summary statistics for strength reduction factor (SRF) results. Hypothesis testing (t-test, F-test, Kolmogorov-Smirnov) used to compare sequential Gaussian approach with alternative methods. t- and F-tests are used to compare if the mean and variance of the two samples originate from the sample population. The Kolmogorov-Smirnov method tests the null hypothesis that the samples are drawn from the same population. All hypothesis testing suggests a statistically significant difference between the sequential Gaussian and alternative approaches with greater than 99% confidence.

Method	Mean	Std. Dev.	n	Std. Error	Hypothesis Test *p*-Valve		
					t-Test	F-Test	Kolmogorov-Smirnov
Sequential Gaussian	1.45	0.08	100	0.01	-	-	-
Zero Autocorrelation	1.53	0.02	100	0.00	<0.01	<0.01	<0.01
Conventional	1.54	0.29	228	0.02	<0.01	<0.01	<0.01
Up-Scaling: Independent	1.35	0.24	100	0.02	<0.01	<0.01	<0.01
Up-Scaling: Dependent	1.33	0.17	100	0.02	<0.01	<0.01	<0.01
Up-Scaling: Roughness	1.33	0.22	100	0.02	<0.01	<0.01	<0.01

variation can be attributed to two factors:

- First, the conventional approach results in a smoother failure surface compared to the SGS method (Figure 15). This is due to the predisposition toward step-path failures within heterogeneous models; whereas, the same phenomenon is not reproduced in homogeneous models, as the nodal similarity in rock mass properties precludes step-path development.
- Second, in conventional probabilistic models, geotechnical domains exhibit a greater influence on failure, compared to individual cells. This is due to the homogeneous assignment of random variables across domains. For example, in heterogeneous models, the averaging of nodal shear strengths along the critical path reduces the influences of outlier deviates; whereas, conventional techniques are susceptible to these outliers due to the homogenous assignment of properties. This issue is discussed in more detailed in Section 6.1.

These two effects result in a fundamental difference in the underlying failure mechanics, resulting in a profound alteration in both the SRF statistics and failure path location.

5.4. No Spatial Autocorrelation

While conventional probabilistic techniques assume perfectly autocorrelated or spatially homogenous domains, the other extreme is to assume no spatial autocorrelation. Under this paradigm, each node is independently simulated, ignoring the influence of nearby cells. To compare SGS methods with this approach, a series of simulations were conducted with an independent GSI and UCS deviate selected for each cell, from the declustered data.

In comparison to the SGS approach, the non-autocorrelated method over-predicts the mean (1.53 vs. 1.45), while at the same time under-estimating the variance (0.02 vs. 0.08; Figure 16; Table 4 and 5). Both effects originate from the reduction in spatial autocorrelation, with the increased mean a result of the lower likelihood of intersecting weaker rock mass clusters and the higher standard deviation due to reduced spatial aggregation. The end effect is an optimistic design, with the probability of unsatisfactory performance under-estimated by several orders of magnitude.

Critical path distribution estimates show a tighter confinement of failure paths within the non-autocorrelated compared to SGS method (Figure 15). The observed variation can be attributed to the decreased clustering of weak rock mass sections in the non-autocorrelated models due to the non-inclusion of the spatial autocorrelation structure. This affects the location of the critical failure path, with increased dispersion observed within the SGS models as the failure path is forced to by-pass the larger clusters of competent

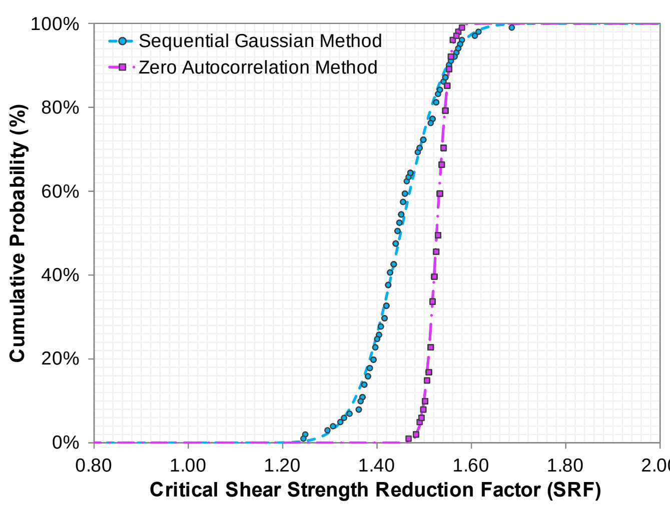

Fig. 16. Incorporation of rock mass strength heterogeneities results in an increased dispersion in the SRF compared to non-autocorrelated models. The zero autocorrelation method is found to overestimate the mean SRF (1.53 vs. 1.45), while at the same time underestimating the standard deviation (0.02 vs. 0.08), when compared to the SGS method.

rock. In comparison, the non-autocorrelated models suppress cluster development resulting in a reduction in critical path deviations. The discrepancy between the models illustrates the need to properly define the spatial structure, as even though both methods have the same attribute statistics, differences in the spatial structure drastically changes the underlying failure path mechanics.

5.5. *Statistical Up-Scaling*

As an alternative to geostatistical simulation, a number of researchers have proposed step-path algorithms to up-scale geotechnical domain statistics (Glynn et al. 1978; Glynn 1979; O'Reilly 1980; Shair 1981; Einstein et al. 1983; Baczynski 2000; Baczynski 2008). The step-path approach was tested through the development of a software package that relies on minimum distance analysis to up-scale geotechnical attributes (Section 4.4). The method calculated summary statistics for the GSI and UCS along critical paths through theoretical rock material. Up-scaled geotechnical attributes were then incorporated into FLAC, and a series of 100 trials conducted for each of the simulations.

Results of the FLAC models suggest that the up-scaling approaches under-estimate the mean SRF, when compared to the SGS method, by approximately 0.11 (Figure 17; Table 4 and 5). The up-scaling approach also drastically over-estimates the SRF variance, resulting in an over-estimation of the probability of failure by approximately seven orders of magnitude. These discrepancies can be attributed to differences in the failure mechanics between the two models. For example, failure within the up-scaled models is found to be preferentially controlled by the weakest domains; whereas, SGS models are predisposed to failure in the weakest cells (Figure 15).

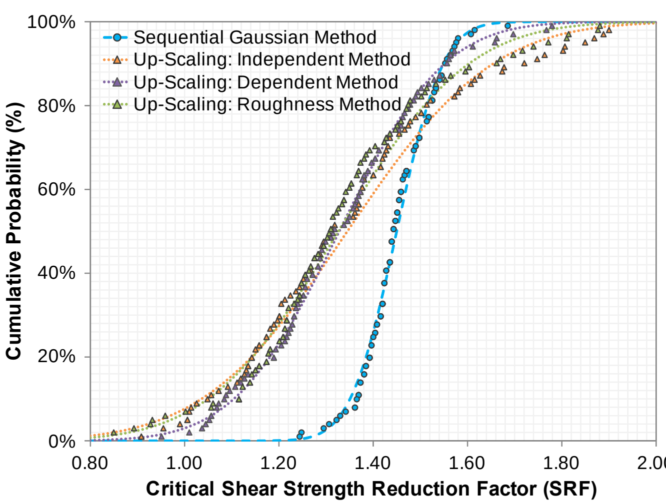

Fig. 17. Comparison of SRF results for the SGS and critical path, upscaling methods. The results suggest the critical path algorithms fail to fully capture the effects of spatial heterogeneity on geomechanical models. Upscaling results suggest a mean SRF of 1.35, 1.33 and 1.33, with a standard deviation of 0.24, 0.17 and 0.22 for the independent, dependent and roughness methods, respectively.

6. DISCUSSION

6.1. *Scale-Dependency Issue*

Geomechanical simulations have highlighted the discrepancies between conventional probabilistic and spatially heterogeneous models. Compared to heterogeneous models, conventional geotechnical slope design under-estimates both the SRF mean and variance. Discrepancies arise due to the method with which geotechnical data is processed and whether or not autocorrelation is taken into consideration (Haining 2003). Autocorrelation results in two intertwined secondary issues which complicate the use of conventional probabilistic methods and invalidate the independence assumption required to use classical statistical approaches. These issues include scale-effects associated with spatial data aggregation, and the preferential accumulation of strain within weaker areas of the rock mass (Gehlke and Biehl 1934; Haining 2003; Jefferies et al. 2008; Lorig 2009).

The spatial data aggregation issue arises from scale dependencies in the sample variance statistic due to a spatial averaging effect, with the variance typically demonstrating an inverse relationship with the scale of study (Gehlke and Biehl 1934; Journel and Huijbregts 1978; Isaaks and Srivastava 1989; Deutsch 2002; Haining 2003). The classic geological example of this phenomenon is the distribution of copper grades at the grain vs. hand sample scales. At the smaller of the two scales, samples exhibit a larger degree of variance, with copper distributions split into two distinct populations (e.g. copper abundant and deficient grains). However, as the scale of study increases, so too does the amount of spatial aggregation. The end effect is a reduction in the sample variance, as results at the hand sample scale reflect an average of copper abundant and deficient grains. While copper grade distributions provide the classic example of this phenomenon, the behaviour is common with other geological attributes. The key importance for geotechnical slope design studies is that the variance at the geotechnical domain scale likely differs from the variance observed at the data collection scale (Isaaks and Srivastava 1989; Deutsch 2002). This presents an important issue for practicing geotechnical engineers, as classic statistical methods ignore this phenomenon (Harr 1996; Duncan 2000; Wiles 2006; Nadim 2007).

The second issue that arises is the preferential accumulation of strain within weaker areas of the rock mass. This preferential behaviour results in a drift in the mean during shifting scales of study (Jefferies et al. 2008; Lorig 2009). The behaviour is demonstrated in classical geotechnical slope design by the development of step-path failures, whereby the rock mass fails within the weakest rock (Jennings 1970; Einstein et al. 1983). In such a case, the global rock mass strength is the summation of shear and/or tensile strengths along this critical path, and not the rock mass as a whole (Glynn 1979; O'Reilly 1980; Baczynski 2000). The end result is a mean strength along the failure path which is lower than the mean strength of the entire mass. Similar effects are observed in groundwater systems, where scale-effects arise from preferential flow along high hydraulic conductivity (K) units, resulting in an upward drift in the mean away from theoretical multi-log-normal predictions (Sánchez-Vila et al. 1996). In addition to statistical effects, discrepancies in the failure dynamics can occur when heterogeneity is explicitly excluded, as conventional approaches result in an over-smoothed failure surface compared to SGS simulations (Figure 15). This can lead to underlying errors, as the behaviour of conventional models are disproportionately controlled by the uniformly applied geotechnical domain attributes, as opposed to step paths along locally weak rock mass sections.

These data aggregation and preferential strain issues result from underlying scale dependencies in the geotechnical attributes. Their spatial behaviour is commonly misrepresented in geotechnical design studies which assume that the statistics of studied attributes is the same at both the borehole and domain scales. However, this research has shown that this can cause erroneous SRF/FOS predictions compared to geostatistical approaches (Figure 14). This presents a fundamental issue for geotechnical slope design as billions of dollars are spent annually on designs which apply conventional approaches. In comparison to traditional design, the utilized SGS method curtails the scale dependency issue through the imposition of a degree of controlled spatial heterogeneity on the random field. The spatial structure is imposed through the use of variograms, which allow for preservation of the sample-scale variance, while at the same time more accurately representing the large-scale, system variance (Journel and Huijbregts 1978). The final result is a more realistic distribution in predicted SRF/FOS results.

6.2. Step-Path Estimation Algorithms

In order to circumvent the aforementioned scale dependency issue, a number of studies have proposed the use of critical path algorithms to up-scale attribute distributions from the borehole to domain scale (Glynn et al. 1978; Glynn 1979; O'Reilly 1980; Shair 1981; Einstein et al. 1983; Baczynski 2000; Baczynski 2008). The applicability of these methods was tested within this study with results suggesting that the critical path approach fails to fully account for the up-scaling issues, and may impart new uncertainties into the analysis (Figure 17). Specifically, failure development within the up-scaled models is found to be controlled by the weakest domains; whereas, failure within the heterogeneous models occurs through preferential failure along the weakest nodes. The overall effect is an over-smoothing of the failure surface within up-scaled models and a reduction in the large-scale roughness (Figure 15).

Attempts to correct for this discrepancy have been made through the calculation of a large-scale roughness factors (Baczynski 2000). However, difficulties arise in calculating the roughness angle as the dominant failure direction often deviates from the average step-path angle, and deep-seated failures can produce quasi-circular geometries resulting in deviating failure directions throughout the sliding mass (Baczynski 2014). As has been shown in this study, simplified calculations of the step-path scale, roughness are currently unable in reproduce the larger-scale step-path behaviour when compared to explicit geostatistical simulation of the spatial heterogeneity. As a result, the use of step-path algorithms remains problematic until/unless a robust method for estimating up-scaled, step-path, roughness coefficients is developed.

6.3. Continuum Mechanics and Data Aggradation

Geomechanical simulation models used throughout this study relied on the use of the Hoek-Brown criterion (Hoek et al. 2002). However, the method has been criticized due to difficulties in applying it to inappropriate conditions (Brown 2008; Mostyn and Douglas 2000; Douglas and Mostyn 2004; Carter et al. 2007; Carvalho et al. 2007; Carter et al. 2008). One of the main issues is the definition of a homogenization scale, as fracture systems research has suggested that many systems display fractal spatial distributions, which preclude the existence of such a scale or representative elementary volume (REV; Bonnet et al. 2001, Mandelbrot 1982; Davy et al. 1990; Davy et al. 1992; Sornette et al. 1993). The REV concept is further complicated by the discrete nature of geotechnical domains, as required scales to achieve an appropriate REV may exceed domain scales (Figure 18).

Comparisons of failure mechanisms from continuum modelling in our study with previous discontinuum modelling at the Ok Tedi site suggest a similar shear-dominated, rotational failure develops using both model approaches (Baczynski et al. 2011). Such behaviour can be attributed to the dense, chaotic fracturing at the Ok Tedi site, which seems to satisfy the primary Hoek-Brown assumption of the rock mass failing from translation and/or rotation of individual blocks (Hoek

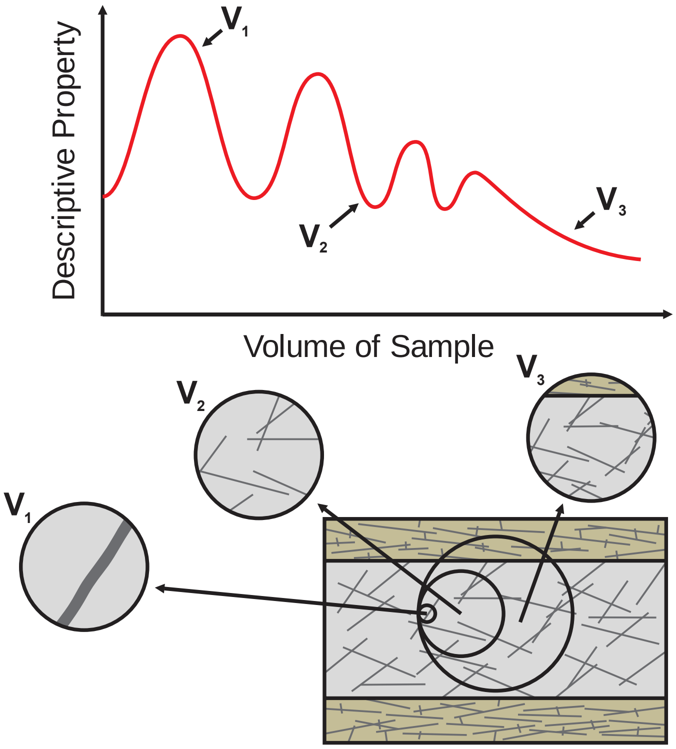

Fig. 18. The discrete nature of geotechnical domains makes the definition of a REV within fracture systems difficult, if not impossible. This is due to the difficulty in stabilizing descriptive attributes at sample volumes smaller than the domain scale.

1983). Despite this, problems may still exist with the Hoek-Brown approach as a result of the spatial aggregation utilized during numerical modelling. Specifically, data was averaged over 10 m3 bins, equivalent to the numerical mesh grid size (Section 4.1.1). The problem with this approach is that it assumes that strain is evenly distributed at the sub-nodal scale. However, as was discussed in the preceding sections, this assumption is invalid due to preferential failure of a rock mass within its weakest areas. These preferential strain accumulations result in the scale effects commonly observed in rock mechanics problems, whereby the compressive strength of a sample is found to be inversely correlated to the sample size (Johns 1966; Bieniawski 1967; Pratt et al. 1972; Hoek and Brown 1980; Bieniawski 1984; de Vallejo and Ferrer 2011). In effect, the SGS models accurately reproduce spatial heterogeneities at the nodal scale, but fail to continue the heterogeneity modelling down to the sub-nodal scale. This imparts an unknown degree of uncertainty into the simulations, which requires further research. As a result, caution is required when extrapolating SRF estimates for risk and/or stability analysis purposes. Despite this limitation, the general conclusions of this study are still considered valid, as the approach was directed at investigating the variation between the methods as opposed to specific SRF values.

7. CONCLUSIONS

The field of geotechnical slope design is currently in a state of flux. Open pit mine operations are progressing towards ever deeper targets in response to the depletion of near surface deposits (Read and Stacey 2009). This increases both costs and uncertainties, forcing geotechnical engineers to reconsider traditional deterministic design techniques (Harr 1996; Duncan 2000; Wiles 2006; Nadim 2007). In the face of these issues, probabilistic design techniques represent an attractive alternative, as uncertainties can be quantified directly within the framework of risk and/or decision analysis (Steffen 1997; Terbrugge et al. 2006; Steffen and Contreras 2007; Steffen et al. 2008). However, conventional probabilistic design techniques typically utilize a discrete geotechnical domain approach, with attributes defined by spatially constant, random variables (Read and Stacey 2009). This can lead to fundamental underlying problems, as spatial dependencies invalidate the sample independence assumption required to use classical statistical approaches, and lead to scale effects due to spatial data aggregation and preferential strain accumulation issues (Gehlke and Biehl 1934; Journel and Huijbregts 1978; Isaaks and Srivastava 1989; Deutsch 2002; Haining 2003; Jefferies et al. 2008; Lorig 2009). Our research on a large open pit slope has demonstrated that failure to consider spatial dependencies in a dataset can result in a fundamental difference in the predicted SRF/FOS results, which is consistent with previous research (Figure 14; Griffiths and Fenton 2000; Hicks and Samy 2002). Discrepancies results from an underlying difference in how the methods handle spatial dependencies inherent in geotechnical databases. In the case of geostatistical approaches, spatial dependencies are accounted for through use of variograms, whereas conventional probabilistic approaches ignore these inherent dependencies and falsely assume data independence. This observation is of specific relevance to geotechnical design studies, as billions of dollars are invested annually, using conventional methods that rely on this incorrect assumption of data independence to formulate probabilistic distributions. Instead, the rigorous application of geostatistical theory is required which explicitly accounts for spatial dependencies inherent in geotechnical data collection. Although the proposed approach is more data intensive and difficult to apply, the inability to account for spatial dependencies in a dataset may lead to systematic errors, invalid results, and poor designs.

ACKNOWLEDGEMENTS

This research was supported by SRK Consulting (Canada) Ltd. and the Natural Sciences and Engineering Research Council of Canada (NSERC) through an NSERC – Industrial Postgraduate Scholarship awarded to John Mayer. The authors would like to thank Diana Allen, Dan Gibson, Norbert Baczynski, Jarek Jakubec, Scott Dunbar and Jennifer Mayer for their reviews of earlier drafts of this manuscript. In addition we thank several colleagues for their support and guidance including Ian de Bruyn, Marek Nowak, Guy Dishaw, and Greg Fagerlund. We would like to acknowledge the generous assistance of Ok Tedi Mining Ltd. for providing the data to conduct this study. Finally, the authors also thank the associate editor and two anonymous reviewers for their helpful comments.

REFERENCES

Abrahams G, Raynor M, and Mandisodza K (2015) Saprolite slope design at the Rosebel Gold Mine. In: Proceedings of Slope Stability 2015: International Symposium on Rock Slope Stability in Open Pit Mining and Civil Engineering, Vancouver, Canada. p 16

Albataineh N (2006) Slope stability analysis using 2D and 3D methods. MSc Thesis, University of Akron

Argumedo AK, Mendive IG, and Sfriso AO (2016) Slope stability analysis at Fenix open pit mine using stochastic finite elements. In: Proceedings of the 15th Congreso Colombiano de Geotechnia & 2nd Conferencia Internacional Especializada en Rocas Blancas, Cartagena, Columbia. p 7

Baczynski NRP (1980) Rock mass characterization and its application assessment of unsupported underground openings. PhD Thesis, University of Melbourne

Baczynski NRP (2000) STEPSIM4 "step-path" method for slope risks. In: Proceedings of GeoEng2000: An International Conference on Geotechnical & Geological Engineering, Melbourne, Australia. pp 19-24.

Baczynski NRP (2008) STEMSIM4-REVISED: Network analysis methodology for critical paths in rock mass slopes. In: Proceedings of the Southern Hemisphere International Rock Mechanics Symposium (SHIRMS-2008), Perth, Australia. pp 13.

Baczynski NRP, de Bruyn I, Mylvaganam J, Walker D (2011) High rock slope cutback geotechnics: a case study at Ok Tedi mine. In: Proceedings of Slope Stability 2011: International Symposium on Rock Slope Stability in Open Pit Mining and Civil Engineering, Vancouver, Canada. pp 14.

Baczynski NRP (2014) Personal Communications. August 22, 2014.

Bieniawski ZT (1967) Mechanism of brittle fracture of rock: parts I – theory of the fracture process. Int J Rock Mech Min Sci Geomech Abstr. 4:395-430

Bieniawski ZT (1976) Rock mass classification in rock engineering. In: Proceedings of the Symposium on Exploration for Rock Engineering, Johannesburg, South Africa. pp 97-106

Bieniawski ZT (1984) Rock mechanic design in mining and tunnelling. Balkema, Rotterdam

Bieniawski ZT (1989) Engineering rock mass classifications. John Wiley & Sons, New York, USA

Blackmore S, Godwin R, Fountas S (2003) The analysis of spatial and temporal trends in yield map data over six years. Biosyst Eng. 84:455-466

Bonnet E, Bour O, Odling NE, Davy P, Main I, Cowie P, Berkowitz B (2001) Scaling of fracture systems in geological media. Am Geophys Union. 39:347-383

Brown ET (2008) Estimating the mechanical properties of rock masses. In: Potvin Y, Carter J, Dyskin A, Jeffery R (eds) SHIRMS 2008, Australian Centre for Geomechanics, Perth, Australia. pp 3-22

Cala M, Flisiak J, and (2006) Slope stability analysis with FLAC in 2D and 3D. In: Proceedings of the 4th International FLAC Symposium on Numerical Modeling in the Geomechanics, Madrid, Spain. p 4

Carter TG, Diederichs MS, Carvalho JL (2007) A unified procedure for Hoek-Brown prediction of strength and post yield behaviour for rock masses at the extreme ends of the rock competency scale. In: Ribeiro e Sousa L, Olalla C, Grossmann N (eds) Proceedings of the 11th Congress of the International Society for Rock Mechanics. pp 161-164

Carter TG, Diederichs MS, Carvalho JL (2008) Application of modified Hoek-Brown transition relationships for assessing strength and post yield behaviour at both ends of the rock competence scale. J S Afr Inst Min Metall. 108:325-338

Carvalho JL, Carter TG, Diederichs MS (2007) An approach for prediction of strength and post yield behaviour for rock masses of low intact strength. In: Eberhardt E, Stead D, Morrison T (eds) Proceedings of the 1st Canada-US Rock Mechanics Symposium, Vancouver, Canada. pp 277-285

Castrignanò A, Buondonno A, Odierna P, Fiorentino C, Coppola E (2009) Uncertainty assessment of soil quality index using geostatistics. Environmetrics. 20:298-311

Cavounidis S (1987) On the ratio of factor of safety in slope stability analyses. Geotech. 37:207-210

Chilés JP, Delfiner P (1999) Geostatistics: Modeling Spatial Uncertainty. 2nd ed. Wiley, New Jersey, USA

Chugh AK (2003) On the boundary conditions in slope stability analysis. Int. J. Numer. Anal. Met. Geomech. 27: 905-926.

Clark I (1979) Practical Geostatistics. 1st ed. Elsevier Applied Science, Essex, UK

Clark WAV, Avery KL (1976) The effects of data aggregation in statistical analysis. Geogr Anal. 75:428-438

Clover Associates Pty Ltd. (2010) GALENA. Version 5.0. Software. Robertson, Australia

Davy P, Sornette A, Sornette D (1990) Some consequences of a proposed fractal nature of continental faulting. Nat. 348:56-58

Davy P, Sornette A, Sornette D (1992) Experimental discovery of scaling laws relating fractal dimensions and the length distribution exponent of fault systems. Geophys Res Lett. 19:361-363

Dawson EM, Roth WH, Dresher A (1999) Slope stability analysis by strength reduction. Géotechnique. 46:835-840

de Bruyn I, Mylvaganam J, Baczynski NRP (2011) A phased modelling approach to identify passive drainage requirements for ensuring stability of the proposed west wall cutback at Ok Tedi mine, Papua New Guinea. In: Proceedings of Slope Stability 2011: International Symposium on Rock Slope Stability in Open Pit Mining and Civil Engineering, Vancouver, Canada. pp 12

de Bruyn I, Coulthard MA, Baczynski NRP, Mylvaganam J (2013) Two-dimensional and three-dimensional distinct element numerical stability analysis for assessment of the west wall cutback design at Ok Tedi Mine, Papua New Guinea. In: Dight PM (eds) Proceedings of Slope Stability 2013: International Symposium on Rock Slope Stability in Open Pit Mining and Civil Engineering, Brisbane, Australia. pp 653-668

de Vallejo LI, Ferrer M (2011) Geological Engineering. CRC Press, Taylor & Francis Group, London, UK

Deutsch CV, Journal AG (1998) GSLIB: Geostatistical Software Library and User's Guide. Oxford University Press, New York, USA

Deutsch CV (2002) Geostatistical reservoir modeling. Oxford University Press, Oxford, UK

DHI-WASY GmbH (2013) FEFLOW: Finite-Element Simulation Systems for Subsurface Flow and Transport Processes. Version 6.2. 64-bit. Software. Berlin, Germany

Diederichs MS, Lato M, Hammah R, Quinn P (2007) Shear strength reduction approach for slope stability analysis. In: Proceedings of the 1st Canada-US Rock Mechanics Symposium, Vancouver, Canada. pp 8

Dijkstra EW (1959) A note on two problems in connexion with graphs. Numerical Mathematics. 1:269-271

Dimitrakopoulos R, Fonseca MB (2003) Assessing risk in grade–tonnage curves in a complex copper deposit, northern Brazil, based on an efficient joint simulation of multiple correlated variables. In: Proceedings of the Application of Computers and Operations Research in the Minerals Industries, Cape Town, South Africa. pp 373–382

Douglas KJ, Mostyn G (2004) The shear strength of rock masses. In: Farquar G, Kelsy, Marsh, Fellows (eds) Proceedings of the 9th Australia New Zealand Conference on Geomechanics, New Zealand Geotechnical Society, Auckland, New Zealand. pp 166-172

Dowd PA (1992) A review of recent developments in geostatistics. Comput Geosci. 17:1481-1500

Duncan JM (2000) Factors of safety and reliability in geotechnical engineering. J Geotech Geoenv Eng. 126:307-316

Einstein HH, Baecher GB (1983) Probabilistic and statistical methods in engineering geology. Rock Mech Rock Eng. 16:39-72

Esfanhani NM, Asghari O (2013) Fault detection in 3D by sequential Gaussian simulation of Rock Quality Designation (RQD). Arab J Geosci. 10:3737-3747

Fagerlund G, Royle M, Scibek J (2013) Integrating complex hydrogeological and geotechnical models – a discussion of methods and issues. Dight PM (eds) Proceedings of Slope Stability 2013: International Symposium on Rock Slope Stability in Open Pit Mining and Civil Engineering, Brisbane, Australia. pp 1091-1102

Gehlke CE, Biehl K (1934) Certain effects of grouping upon the size of correlation coefficient in census tract material. J Am Stat Assoc Suppl. 29:169-170

Glynn EF, Veneziano D, Einstein HH (1978) The probabilistic model for shearing resistance of jointed rock. In: Proceedings of the 19th US Symposium on Rock Mechanics (USRMS). American Rock Mechanics Association. pp 66-76

Glynn E (1979) A probabilistic approach to the stability of rock slopes. PhD dissertation, Massachusetts Institute of Technology

Goovaerts P (1997) Geostatistics for Natural Resources Evaluation. 1st ed. Oxford University Press, New York

Griffiths DV, Fenton GA (2000) Influence of soil strength spatial variability on the stability of an undrained clay slope by finite elements. In: Proceedings of GeoDenver 2000, Denver, ASCE Geotechnical Special Publication No. 101, 184-193. New York. DOI:10.1061/40512(289)14

Haining RP (2003) Spatial data analysis: theory and practice. Cambridge University Press, Cambridge, UK

Hallin M, Lu Z, Tran LT (2004) Kernel density estimation for spatial processes: the L1 theory. J Multivar Anal. 88:61-75

Hammah RE, Yacoub TE, Corkum B, Curran J (2005) The shear strength reduction method for the generalized Hoek-Brown criterion. In: Proceedings of the 40th U.S. Symposium on Rock Mechanics, Anchorage, USA. pp 6

Hammah RE, Yacoub TE, Curran JH (2006) Investigating the performance of the shear strength reduction (SSR) method on the analysis of reinforced slopes. In: Proceedings of the 59th Canadian Geotechnical Conference, Vancouver, Canada. pp 5

Harr ME (1996) Reliability based design in civil engineering. Dover, New York, USA

Hearn GJ (1995) Landslide and erosion hazard mapping at Ok Tedi copper mine, Papua New Guinea. Q J Eng Geol Hydrogeol. 28:47-60

Hicks MA, Samy K (2002) Influence of heterogeneity on undrained clay slope stability. Q J Eng Geol Hydrogeol. 35:41-49

Hoek E, Brown ET (1980) Underground excavations in rock. 1st edition. Institute of Mining and Metallurgy, London, UK

Hoek E (1983) Strength of jointed rock masses. Géotechnique. 23:187-223

Hoek E (1994) Strength of rock and rock masses. ISRM News Journal. 2:4-16

Hoek E, Kaiser PK, Bawden WF (1995) Support of Underground Excavations in Hard Rock. Balkema, Rotterdam, Netherlands

Hoek E, Kaiser PK, Bawden WF (1997) Practical estimates of rock mass strength. Int J Rock Mech Min Sci Geomech Abstr. 34:1165-1186

Hoek E, Carranza-Torres C, Corkum B (2002) Hoek–Brown failure criterion-2002 edition. In: Proceedings of the 5th North American Rock Mechanics Symposium, Toronto, Canada. pp 7

Hoek E, Marinos P (2007) A brief history of the development of the Hoek–Brown failure criterion. Soil Rocks. No 2, November. p 13

Hoek E (2012) Blasting damage in rock. Retrieved on December 8, 2012. www.rocscience.com. p 11

Hormazabal E, Veramendi R, Barrios J, Zuñiga G, and Gonzalez F. 2013. Slope design at Cuajone pit, Peru. In: Proceedings of Slope Stability 2011: International Symposium on Rock Slope Stability in Open Pit Mining and Civil Engineering, Vancouver, Canada. p 14

Isaaks EH, Srivastava RM (1989) An Introduction to Applied Geostatistics. 1st ed. Oxford University Press, New York, USA

Itasca Consulting Group Inc. (2011) FLAC (Fast Lagrangian Analysis of Continua). Version 7.00.411. Software. Minneapolis, USA

Itasca Consulting Group Inc. (2014) UDEC (Universal Distinct Element Code). Version 6.00.282. Software. Minneapolis, USA

Jakubec J, Laubscher DH (2000) The MRMR rock mass rating classification system in mining practice. In: Proceedings of the 3rd International Conference and Exhibition on Mass Mining, Brisbane, Australia. pp 413-421

Jefferies M, Lorig L, Alvarez (2008) Influence of rock-strength spatial variability on slope stability. In: Hart R, Detournay C, Cundall P (eds) Proceedings of Continuum and Distinct Element Numerical Modeling in Geo-Engineering, Itasca Consulting Group, Minneapolis, USA. Paper 01-05. pp 9

Jennings J (1970) A mathematical theory for the calculation of the stability of slopes in open cast mines. In: Proceeding of the Symposium on the Theoretical Background to the Planning of Open Pit Mines, Johannesburg, South Africa. pp 87-102

Jenson OP, Christman MC, Miller TJ (2006) Landscape-based geostatistics: a case study of the distribution of blue crab in Chesapeake Bay. Environmetrics. 17:605-621

Jiang X, Qiu Y, Wei Y, and Ling J (2008) Application of SSRM in stability analysis of subgrade embankment over sloped weak ground with FLAC3D. In: Proceedings of the 10th International Symposium on Landslide and Engineered Slopes Taylor & Francis, Xian, China. p 6

Johns H (1966) Measuring the strength of rock in situ at an increasing scale. In: Proceedings of the 1st ISRM Congress, Lisbon, Portugal. pp 477-482

Journel AG, Huijbregts CJ (1978) Mining Geostatistics. 1st ed. Academic Press, New York, USA

Laubscher DH (1990) A geomechanics classification system for the rating of rock mass in mine design. J S Afr Inst Min Metall. 90:257-273

Laubscher DH, Jakubec J (2001) The MRMR rock mass classification for jointed rock masses. In: Hustrulid WA, and Bullock RL (eds) Underground mining methods: engineering fundamentals and international case studies, Society of Mining Metallurgy and Exploration, Littleton, USA. pp 475-481

Leuangthong O, Khan KD, Deutsch CV (2011) . Solved problems in geostatistics. 2nd ed. Wiley, New Jersey, USA

Little T (1999) The reliability of blast damaged slopes, In: Proceedings of the 5th Australasian Institute of Mining and Metallurgy EXPLO 99 Conference, Melbourne, Australia. p 9

Li AJ, Merifield RS and Lyamin SV (2011) Effect of rock mass disturbance on the stability of rock slopes using the Hoek–Brown failure criterion. Comput. Geotech. 38:546–558

Lorig LJ (2009) Challenges in current slope stability analysis methods. In: Proceedings of Slope Stability 2009: International Symposium on Rock Slope Stability in Open Pit Mining and Civil Engineering, Santiago, Chile. p 8

Lupogo K, Tuckey Z, Stead D, and Elmo D (2014) Blast damage in rock slopes: potential applications of discrete fracture network engineering. In: Proceedings of the 1st International Discrete Fracture Network Engineering Conference, Vancouver, Canada. p 14

Mandelbrot BB (1982) The fractal geometry of nature. W.H. Freeman, New York, USA

Matheron G (1963) Principles of geostatistics. Economic Geology. 58:1246-66

Mattsui T, San KC (1992) Finite element slope stability analysis by shear strength reduction technique. Soil Found. 32:59-70

Mostyn G, Douglas K (2000) Strength of intact rock and rock masses. In: Proceedings of GeoEng 2000, Technomic Publishing Company, Lancaster, USA. pp 1389-1421

Nadim F (2007) Tools and strategies for dealing with uncertainty in geotechnics. In: Griffiths DV, Fenton GA (eds) Probabilistic Methods in Geotechnical Engineering. CISM Courses and Lectures No. 491, Springer, New York, USA. pp 71-95

Nowak M, Verly G (2004) The practice of sequential Gaussian simulation. In: Leuangthong O, Deutsch CV (eds) Geostatistics Banff, Netherlands, Springer. pp 387-398

Nowak M, Verly G (2007) A practical process for geostatistical simulation with emphasis on Gaussian methods. In: Dimitrakopoulos R (eds) Orebody Modelling and Strategic Mine Planning - Uncertainty and Risk Management Models. 2nd Edition. The Australasian Institute of Mining and Metallurgy (The AusIMM). pp 10

O'Reilly K (1980) The effect of joint plane persistence on rock slope reliability. MSc Thesis, Massachusetts Institute of Technology

Page RW (1975) Geochronology of Late Tertiary and Quaternary mineralised intrusive porphyries of the Star Mountains of Papua New Guinea and Irian Jaya. Econ Geol. 70:928-936

Pascoe DM, Pine RJ, Howe JH (1998) An extension of probabilistic slope stability analysis of china clay deposits using geostatistics. In: Maund JG, Eddleston M (eds) Geohazards in Engineering Geology. Geological Society. Engineering Geology Special Publications, London, UK. 15:193-197

Phillips DL, Dolph J, Marks D (1992) A comparison of geostatistical procedures for spatial analysis of precipitation in mountainous terrain. Agric For Meteorol. 58:119-141

Pratt HR, Black A, Brown W, Brace W (1972) The effect of specimen size on the mechanical properties of unjointed diorite. Int J Rock Mech Min Sci Geomech Abstr. 9:513-516

Prycz MJ, Deutsch CV (2003) Declustering and debiasing. In: Searston S (eds) Newsletter 19. Geostatistical Association of Australasia, Melbourne, Australia. pp 25

Read JRL (2009) Data uncertainty. In: Proceedings of Slope Stability 2009: International Symposium on Rock Slope Stability in Open Pit Mining and Civil Engineering, Santiago, Chile. pp 6

Read JRL, Stacey P (2009) Guidelines for open pit slope design. 1st ed. CSIRO, Collingwood, Australia

Rocscience Inc. (2014) Slide. Version 6.029. Software. Toronto, Canada.

Sánchez-Vila X, Carrera J, Girardi JP (1996) Scale effects in transmissivity. J Hydrogeol. 183:1-22

Shair A (1981) The effect of two sets of joints on rock slope reliability. MSc Thesis, Massachusetts Institute of Technology

Sornette A, Davy P, Sornette D (1993) Fault growth in brittle-ductile experiments and the mechanics of continental collisions. J Geophys Res. B7:12111-12139

Srivastava RM, Parker HM (1989) Robust measures of spatial continuity. In: Armstrong M (eds) Geostatistics, Kluwer Academic Publishers, Alphen aan den Rijn, Netherlands. pp 295-308

Srivastava A (2012) Spatial variability modelling of geotechnical parameters and stability of highly weathered rock slope. Indian Geotech J. 42:179-185

SRK Consulting (Australasia) Pty Ltd. (2012) Comparison of Laubscher and Bieniawski RMR values. Internal Report Prepared for Ok Tedi Mining Ltd. Perth, Australia. pp 7

Steffen OKH (1997) Planning of open pit mines on a risk basis. J S Afr Inst Min and Metall. 97:47-56

Steffen OKH, Contreras LF (2007) Mine planning-its relationship to risk management. In: Proceedings of the International Symposium on Stability of Rock Slopes in Open Pit Mining and Civil Engineering, Perth, Australia. pp 17

Steffen OKH, Contreras LF, Terbrugge PJ, Venter J (2008) A risk evaluation approach for pit slope design. In: Proceedings of the 42nd US Rock Mechanics Symposium and 2nd US-Canada Rock Mechanics Symposium, San Francisco, USA. pp 18

Styles T (2015) Application of Blast Damage when Modelling Open Pit Slopes. In: Proceedings of the Mineral and Metals Production from Mine to Market, Cambridge, UK.

Terbrugge PJ, Wesseloo J, Venter J, Steffen OKH (2006) A risk consequence approach to open pit slope design. J S Afr Inst Min and Metall. 106:503-511

Tuckey Z, Justine P, and Price J (2016) Discontinuity survey and brittle fracture characterisation in open pit slopes using photogrammetry. In: Proceedings of the 1st Asia Pacific Slope Stability in Mining Conference, Brisbane, Australia. p 15

Vann J, Bertoli O, Jackson S (2002) An overview of geostatistical simulation for quantifying risk. In: Proceedings of Geostatistical Association of Australasia Symposium Quantifying Risk and Error, Perth, Australia. pp 12

Vieira SR, Hatfield TL, Nielsen DR, Biggar JW (1983) Geostatistical theory and application to variability of some agronomical properties. Hilgardia. 51:1-75

Vieira SR, Millete J, Topp GC, Reynolds WD (2002) Handbook for geostatistical analysis of variability in soil and climate data. In: Alvarezz VH, Schaefer CR, Barros NF, Mello JWV, Costa LM (eds) Tópicos em Ciência do solo. Viçosa: Sociedade Brasileira de Ciência do solo. 2:1-45

Vieira SR, Carvalho JRPD, Ceddia MB, González AP (2010) Detrending non stationary data for geostatistical applications. Bragantia. 69:01-08

Wen A, Sturzenegger M, and Stead D (2015) Analysis of a Complex Rock Slope Instability with a Stepped Failure Surface using Discrete Fracture Network Models. In: Proceedings of the 1st International Discrete Fracture Network Engineering Conference, Vancouver, Canada. p 10

Wiles TD (2006) Reliability of numerical modelling predictions. Int J Rock Mech Min Sci Geomech Abstr. 43:454-472

Wolter A, Gischig V, Stead D, and Clague JJ (2015) Investigation of Geomorphic and Seismic Effects on the 1959 Madison Canyon, Montana, Landslide Using an Integrated Field, Engineering Geomorphology Mapping, and Numerical Modelling Approach. Rock Mech Rock Eng. 49:2479-2501

Yoe C (2011) Primer on risk analysis. Taylor & Francis Group, London, UK

Yule AU, Kendall MG (1950) An introduction to the theory of statistics. Hafner Publishing Company, New York, USA